

MEMBRANE SEPARATION IN SUPERCRITICAL ANTISOLVENT PROCESS FOR
NANOPARTICLE PRODUCTION

Except where reference is made to the work of others, the work described in this thesis is my own or was done in collaboration with my advisory committee. This thesis does not include proprietary or classified information.

Kayoko Ono

Certificate of Approval:

W. Robert Ashurst
Assistant Professor
Chemical Engineering

Ram B. Gupta, Chair
Professor
Chemical Engineering

Yoon Y. Lee
Professor
Chemical Engineering

Joe F. Pittman
Interim Dean
Graduate School

MEMBRANE SEPARATION IN SUPERCRITICAL ANTISOLVENT PROCESS FOR
NANOPARTICLE PRODUCTION

Kayoko Ono

A Thesis

Submitted to

the Graduate Faculty of

Auburn University

in Partial Fulfillments of the

Degree of

Master of Science

Auburn, Alabama
December 15, 2006

MEMBRANE SEPARATION IN SUPERCRITICAL ANTISOLVENT PROCESS FOR
NANOPARTICLE PRODUCTION

Kayoko Ono

Permission is granted to Auburn University to make copies of this thesis at its discretion, upon request of individuals or institutions and at their expense. The author reserves all publications rights.

Signature of Author

Date of Graduation

VITA

Kayoko Ono, daughter of Hatsuo and Remiko Ono, was born September 22, 1981, in Kumamoto prefecture, Japan. She graduated from Seiseiko High School in March, 2000. She entered Tohoku University in Sendai, Japan in April, 2000 and graduated with a Bachelor of Engineering (Applied Chemistry) in March, 2004. In August, 2004, she entered the Graduate School, Auburn University, in Auburn, Alabama to pursue MS degree in Chemical Engineering.

THESIS ABSTRACT

MEMBRANE SEPARATION IN SUPERCRITICAL ANTISOLVENT PROCESS FOR
NANOPARTICLE PRODUCTION

Kayoko Ono

Master of Science, December 2006
(B.S., Tohoku University, Sendai, 2004)

103 Typed Pages

Directed by Ram B. Gupta

In supercritical antisolvent process to produce pharmaceutical nanoparticles, drug solution is injected into supercritical carbon dioxide. CO₂ rapidly extracts the solvent, causing the drug to precipitate as micro- and nano-particles. A portion of drug dissolves in CO₂/organic solvent mixture. For the recovery of drug nanoparticles from the precipitation vessel, CO₂/organic solvent is removed through a filter. As much as 50% of the drug is typically lost in the process, in dissolved and un-retained particle forms. Hence a better method to separate CO₂/organic solvent is needed. In this work, a polymer membrane based separation of CO₂/organic solvent is proposed and tested.

Gas and vapor separations using non-porous polymer membranes have been brought to focus in the past 30 years. Very recently, amorphous Teflon (TeflonAF,

DuPont, Wilmington, DE) polymers have been introduced which are copolymers consisting of 2,2-bis(trifluoromethyl)-4,5-difluoro-1,3-dioxole (PDD) and tetrafluoroethylene (TFE). Teflon AF 2400 contains 87 mol% PDD and 13 mol% TFE with $T_g = 240\text{ }^\circ\text{C}$, whereas Teflon AF 1600 contains 65 mol% PDD and 35 mol% TFE with $T_g = 160\text{ }^\circ\text{C}$. Both the copolymers have a high temperature stability and chemical resistance, as well as high free volume compared to the conventional glassy polymers. Permeability coefficients of CO_2 in Teflon AF 2400, Teflon AF 1600, and poly(tetrafluoroethylene) (PTFE) are measured, at varying feed pressure and temperature. The permeability increased in the order of $\text{PTFE} < \text{Teflon AF 1600} < \text{Teflon AF 2400}$. This can be explained by the fact that PTFE is a semicrystalline polymer and Teflon AFs are glassy polymers with a high free volume. In addition, the reuse of the membrane for second and third time resulted in enhancement of the permeability, which can be attributed to the CO_2 plasticization of the membrane. Further understanding of the transport of CO_2 through the membranes is investigated by applying solution-diffusion model. In the presence of CO_2 , acetone solvent has a high permeability through Teflon AF. And no permeability of larger drug molecule tetracycline is observed through Teflon AF when dissolved in acetone.

ACKNOWLEDGEMENT

The author would like to thank Prof. Ram B. Gupta for guiding this research work. The work would not have been completed without his advice. Also, gratitude is given toward my colleagues for their advice and help. Last but not least, thanks are due to my parents and my friends, Irais, Suhaila, Zahra and Ken'ichi for their support.

TABLE OF CONTENTS

CHAPTER 1: INTRODUCTION	1
CHAPTER 2: AMOURPHOUS TEFLON MEMBRANE	27
CHAPTER 3: EXPERIMENTAL METHODS	34
CHAPTER 4: PERMEABILITY OF CARBON DIOXIDE	55
CHAPTER 5: PERMEABILITY OF ACETONE	68
CHAPTER 6: PERMEABILITY OF TETRACYCLINE	86
CONCLUSIONS	87
REFERENCES	89

LIST OF FIGURES

Fig. 1-1. Phase diagram of carbon dioxide	1
Fig. 1-2. Density dependence of carbon dioxide	2
Fig. 1-3. Schematic of rapid expansion of supercritical solution (RESS)	3
Fig. 1-4. Schematic of supercritical antisolvent (SAS) Process	4
Fig. 1-5. Amorphous and crystalline portion in a polymer	6
Fig. 1-6. Chemical structures of elastomers	7
Fig. 1-7. Chemical structure of high free volume glassy polymer (PTMSP)	8
Fig. 1-8. Chemical structure of polytetrafluoroethylene (PTFE)	10
Fig. 1-9. Schematic of molecules transporting through a nonporous membrane	12
Fig. 1-10a. Sorption isotherm for gases in elastomers	13
Fig. 1-10b. Sorption isotherm for organic vapor/liquids in polymers	14
Fig. 1-10c. Sorption isotherm for gases in glassy polymers	15
Fig. 1-11. Schematic of sorption isotherms for dual sorption theory	16
Fig. 1-12a. Schematic of constant pressure/variable volume method	23
Fig. 1-12b. Schematic of constant volume/variable pressure method	23
Fig. 1-13. Schematic of a SAS process with membrane separation	25
Fig. 2-1. Chemical structure of Teflon AF products	27
Fig. 2-2. Micrograph of Teflon AF 2400 taken by SEM	28
Fig. 3-1. Schematic of the membrane set-up for CO ₂ permeation	35

Fig. 3-2a. An example of a plot of permeate pressure vs time	38
Fig. 3-2b. An example of a plot of $\ln(p_{\text{feed}}-p_{\text{permeate}})$ vs time	38
Fig. 3-3. Schematic of the set-up for verification of the system	39
Fig. 3-4a. Schematic of the membrane-set up for acetone + CO ₂ permeation	46
Fig. 3-4b. Enlargement of the schematic of the membrane holder	46
Fig. 3-5. Schematic of the tetracycline permeation test	54
Fig. 4-1a. Permeate pressure vs time for CO ₂ permeation	57
Fig. 4-1b. Logarithm of the pressure difference vs time for CO ₂ permeation	57
Fig. 4-2. CO ₂ permeability in Teflon AF 2400, AF1600 and PTFE	60
Fig. 4-3a. Temperature dependence of CO ₂ permeability in Teflon AF 2400	64
Fig. 4-3b. Arrhenius plot of CO ₂ permeability in Teflon AF 2400 film	65
Fig. 4-4a. Plasticization effect on CO ₂ permeability in Teflon AF 2400	66
Fig. 4-4b. Plasticization effect on CO ₂ permeability in Teflon AF 1600	67
Fig. 5-1. Acetone calibration curve	69

LIST OF TABLES

Table 1-1. Glass transition temperature of polymers	8
Table 1-2. Solubility of gases in natural rubber	19
Table 2-1. CO ₂ permeability in various polymers studied previously	32
Table 2-2. CO ₂ Permeability in Teflon AF 2400 studied previously	33
Table 4-1. CO ₂ permeability in Teflon AF 2400, AF 1600 and PTFE	59
Table 4-2. CO ₂ Permeability coefficients in Teflon AF 2400	63
Table 5-1. Verification of set-up for acetone + CO ₂ permeation	74
Table 5-2. Acetone permeation through Teflon AF 1600	77
Table 5-3. Acetone permeability coefficient in Teflon AF 1600	85

CHAPTER 1
INTRODUCTION

Supercritical Fluids

A fluid is supercritical when it is compressed beyond its critical pressure and heated beyond its critical temperature. For example, carbon dioxide is supercritical if it is heated above 31.1 °C and simultaneously compressed above 72.8 atm. The supercritical region can be depicted as shows in Fig. 1-1.

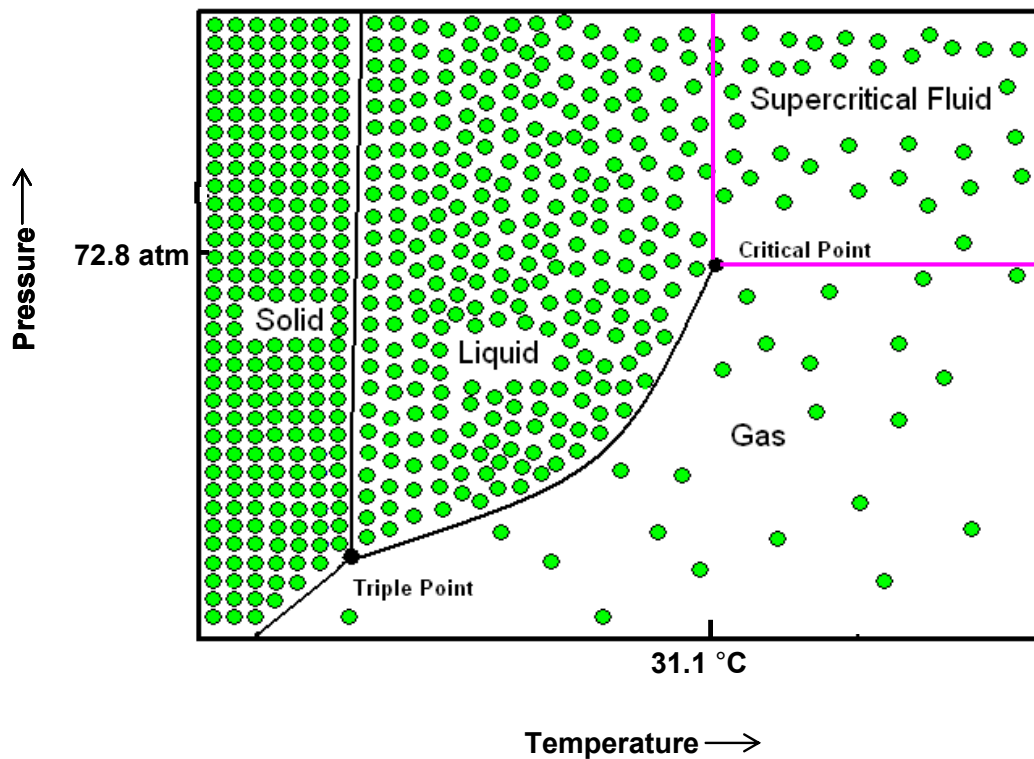


Fig. 1-1. Phase diagram of carbon dioxide.

No amount of compression can liquefy the supercritical fluid. In fact pressure can be used to continuously change the density from gas-like conditions to liquid-like conditions. Near the critical region, small changes in the pressure can give rise to large changes in the density. Fig. 1-2 shows how density of carbon dioxide is varied by pressure at different isotherms.

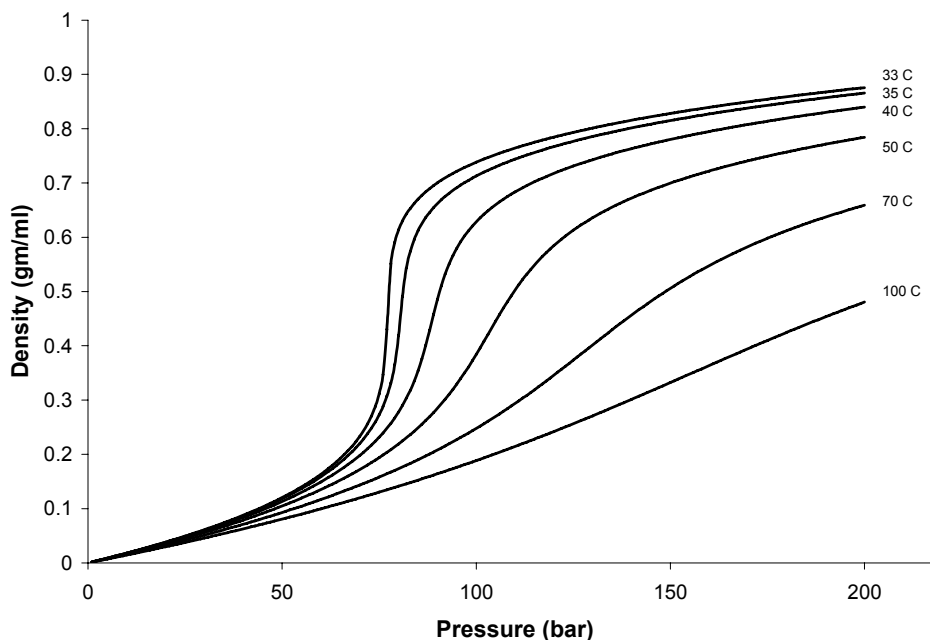


Fig. 1-2. Density dependence of carbon dioxide.

In addition to density, diffusivity of the supercritical fluids is higher than that of liquid solvents, and can be easily varied. For typical conditions, diffusivity in supercritical fluids is of the order of 10^{-3} cm^2/s as compared to 10^{-1} for gases and 10^{-5} for liquids. Typical viscosity of supercritical fluids is of the order of 10^{-4} $\text{g}/\text{cm}\cdot\text{s}$, similar to that of gases, and about 100 fold lower than that of liquids. High diffusivity and low viscosity provide rapid equilibration of the fluid to the mixture. As a supercritical fluid, CO_2 is

often used due to its low critical temperature and pressure as well as its availability and benign character.

Over the past two decades, supercritical carbon dioxide (above 31.1 °C and 72.8 atm) has emerged as a medium for the formation of micro- and nano-particles of pharmaceutical compounds, due to its adjustable solvent properties, high diffusivity, non-flammability, and non-toxicity. Depending upon the solubility in supercritical CO₂, two classes of processes have emerged: (a) rapid expansion of supercritical solution (RESS) for CO₂-soluble materials, and (b) supercritical antisolvent (SAS) for CO₂-insoluble materials.

Schematic of RESS process is shown in Fig. 1-3. In RESS process, the drug material is first dissolved in supercritical CO₂ and then expanded through a nozzle to rapidly precipitate as particles. Since the expansion occurs as fast as the speed of sound, the material comes out as small microparticles. But due to the limited solubility of drugs in supercritical CO₂, RESS process had limited utility so far. In a recently developed RESS-SC process [Thakur and Gupta, 2006] by using menthol solid co-solvent, the solubility has been enhanced by several hundred fold. The presence of the solid cosolvent also hinders the particle growth; hence the particles in nanometer size range are easily obtained. Menthol is later removed by sublimation, yielding pure drug nanoparticles.

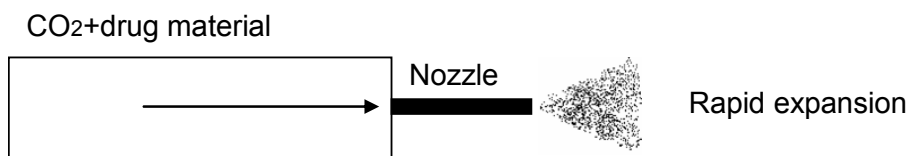


Fig. 1-3. Schematic of rapid expansion of supercritical solution (RESS)

Schematic of an experimental set-up for a SAS process is shown in Fig. 1-4. In SAS process, the drug material is first dissolved in an organic solvent. The solution is then injected into supercritical CO₂, resulting in the extraction of solvent by supercritical CO₂ and precipitation of the material. Since the speed of extraction is fast due to the high (gas-like) diffusivity of supercritical CO₂, the small microparticles of the material are obtained. Recently, the extraction speed was enhanced by ultrasonic mixing which results in nanoparticles [Gupta and Chattopadhyay, 2003]. In the new process, the particle size is easily controlled by the extent of ultrasonic power supplied. The strong extraction ability of supercritical CO₂ allows the production of pure drug nanoparticles, free of any residual solvent or additives.

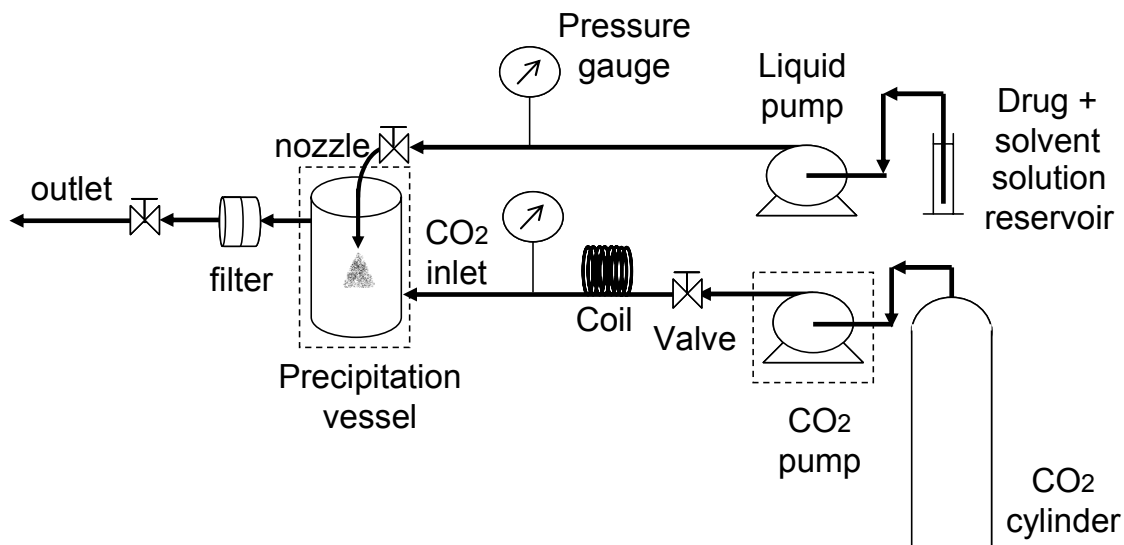


Fig. 1-4. Schematic of supercritical antisolvent (SAS) process

Supercritical fluid processing has been applied to a wide variety of compounds [Arai et al., 2002; Yeo et al., 2004]. However, in these processes, low yield of particle collection has been a problem [Taylor, 1996, Yeo et al., 2004]. This is mainly due to the

failure in separating the particles or dissolved material from the CO₂/solvent mixture. The material loss is a great disadvantage considering the expensive price of many drugs. In addition, pressurization of supercritical fluid, in many cases CO₂, is costly especially looking at it on an industrial scale [Carlson et al., 2005; Bolzan et al., 2001]. Meanwhile, in the field of gas and vapor separations, use of polymer membranes has been brought to focus in the past 30 years and has been investigated heavily since [Mulder, 1996]. There are several researches that have combined these two prevailing technologies: supercritical fluid processing and membrane technology.

Membrane Technology

Polymer as a membrane

A membrane is a barrier used to separate two or more components. Membranes can be made from different materials. It can be from natural or synthetic materials. Synthetic membranes can be either organic or inorganic. Inorganic membranes can be ceramics (alumina, zirconia, titania, etc.), glass membranes made from silica and zeolites. Organic membranes are polymers which is a macromolecule whose basic unit is called a monomer. The monomers build up to make a large chain resulting in large molecular weight. A polymer that consists of one type of monomer is called a homopolymer, whereas a polymer that consists of two or more types of monomers is called a copolymer. When the monomers are sequenced in a random way, the copolymer is called a random copolymer.

Polymers have a portion at which the molecular segments are lined up and a portion at which they are placed randomly (Fig. 1-5). A polymer that contains a large portion of crystalline region is called a (semi-) crystalline polymer. On the other hand, a polymer that has no crystalline portion is called an amorphous polymer. Heating a solid amorphous polymer would change the state of the polymer. As the heat is added, segments in the amorphous region start vibrating and as a result, free volume increases. Free volume refers to the void volume that is not occupied by the polymer chains. The temperature at which this occurs is called a glass transition temperature (T_g) and the state after the transition is called a rubbery state. Polymers that are in the rubbery state at ambient condition, i.e. polymers that have a glass transition temperature below the ambient temperature are called elastomers. Polyethylene (PE) and polydimethylsiloxane (PDMS; silicon rubber) are examples of elastomers (Fig. 1-6).

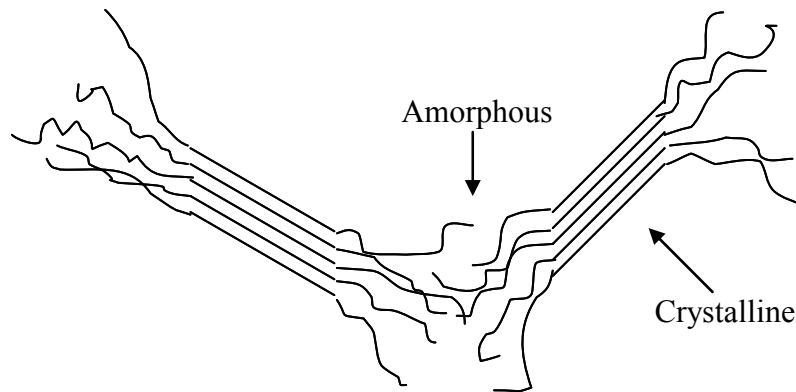
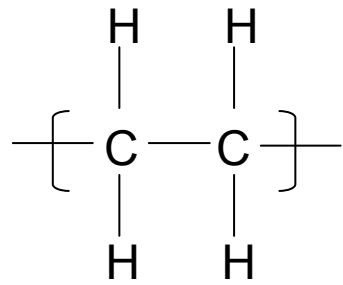
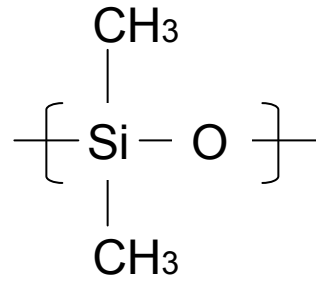


Fig. 1-5. Amorphous and crystalline portion in a polymer



Polyethylene (PE)



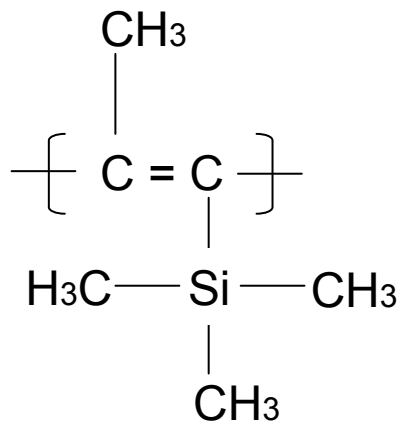
Polydimethylsiloxane (PDMS; silicon rubber)

Fig. 1-6. The chemical structures of the elastomers

Table 1-1 shows the glass transition temperature of some of the polymers. In the glassy state, free volume does not change with temperature, but in the rubbery state, free volume increases as the temperature increases. Since for rubbery polymers, polymer flexibility increases due to the vibrating motion, free volume is increased and hence, most rubbery polymers (elastomers) have larger permeabilities than glassy polymers. However, the highest permeability measured so far is for polytrimethylsilylpropyne (PTMSP), which is a high free-volume glassy polymer (Fig. 1-7). Many research have been conducted to learn the permeation properties of this highly permeable polymer.

Table 1-1. Glass transition temperature of polymers (Schouten, 1987)

Polymer	Glass transition temperature (T _g) [°C]
Polydimethylsiloxane (PDMS)	-123
Polyethylene (PE)	-120
Natural rubber	-72
Polystyrene	100
Polytetrafluoroethylene (PTFE)	126
Polyetheretherketone (PEEK)	143
Polycarbonate	150
Polysulfone	190
Polyimide (Kapton)	300



Poly 1-trimethylsilyl-1-propyne (PTMSP)

Fig. 1-7. Chemical structure of a high free volume glassy polymer (PTMSP)

Free volume can be quantified by a measure called fractional free volume, FFV:

$$\text{FFV} = \frac{V - V_0}{V}$$

where V is the molar volume and V_0 the volume occupied by the polymer chains. V can be calculated by dividing the MW of the polymer by the density which can be determined experimentally.

$$V = \frac{MW}{\rho}$$

V_0 can be calculated using Bondi [1968]'s approximation which is as follows:

$$V_0 = 1.3 \times V_w$$

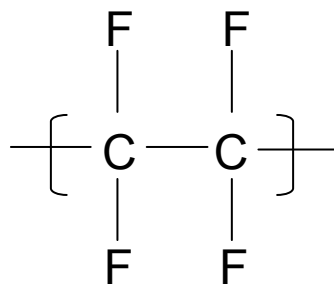
where V_w is the van der Waals volume. V_w can be calculated using a group contribution method [Krevelen, 1990]. Bos et al. [1999] measured free volume on several polymers such as polysulfone, polyethersulfone, polyetherimide, polycarbonate, polyimide (Matrimid 5218), etc. The values ranged from 0.138 to 0.225 with Matrimid the largest value.

Porous and nonporous membranes

In terms of the pore size, membranes can be classified into two: porous and nonporous membranes. Pores exist in nonporous membranes, but their sizes are of a molecular scale and a lot smaller than those of the porous membranes. In general, membranes that have pore size of less than 5-6 Å are considered nonporous, and membranes with pore sizes larger than those are considered porous. 5-6 Å is about the

size of simple molecules. From a statistical point of view, membranes that have fixed pores would be porous and membranes that have pores that appear and disappear transiently would be nonporous.

Porous membranes are used for microfiltration and ultrafiltration. Microfiltration is the separation done in the range of 0.1-10 μm and ultrafiltration is in the range of 2-100 nm (0.002-0.1 μm). Porous membranes contain fixed pores larger than those of the nonporous membranes. The main problem in micro/ultrafiltration is flux decline due to concentration polarization, adsorption, pore-plugging and gel-layer formation [Mulder, 1996]. Examples of polymers for microfiltrations are polycarbonate, polytetrafluoroethylene (PTFE), polypropylene, polyamide, cellulose-ester, polysulfone (PSf), and polyetheretherketone (PEEK). Polytetrafluoroethylene (PTFE) is a hydrophobic material which is highly crystalline and has a high thermal stability and chemical resistance, originally developed by DuPont with Teflon trademark. The chemical structure of PTFE is shown in Fig. 1-8.



Polytetrafluoroethylene (PTFE)

Fig. 1-8. Chemical structure of polytetrafluoroethylene (PTFE)

When the sizes of the molecules are small and are in the same order of magnitude, porous membranes cannot do the separation and nonporous membranes should be used. Hence, nonporous membranes are used in gas/vapor separation and pervaporation. Pervaporation is a liquid permeation method having vacuum at the permeate-side, where the permeants immediately evaporate as vapor.

Insight into the transport mechanism through membranes is needed to determine the performance of the membrane. For porous membranes, several models such as Knudsen flow and Hagen-Poiseuille flow exist [Mulder, 1996]. Knudsen flow is applied when the pores are small compared to the mean free path of the penetrants. Mean free path is the average distance a molecule travel before colliding into another molecule. Hence, in a Knudsen flow, interaction between the molecule and the pore wall is greater than the interaction between the molecules. On the other hand, Hagen-Poiseuille flow, which is also called the viscous flow, is applied when the pores are larger compared to the mean free path, indicating that the interaction between the molecules is greater than that of the molecule and the pore wall. Patil et al. [2006] measured permeation of supercritical CO₂ through polymeric hollow fiber membranes and reached the conclusion that the permeation profile followed Hagen-Poiseuille model.

For nonporous membranes, solution-diffusion model is employed. Since in this work, nonporous membrane is used, transport through nonporous membranes will be discussed in depth by following the solution-diffusion model.

Transport mechanism through nonporous membranes

Transport through nonporous membranes depends on the membrane material. The schematic of molecules transporting through a nonporous (dense) membrane is shown in Fig. 1-9.

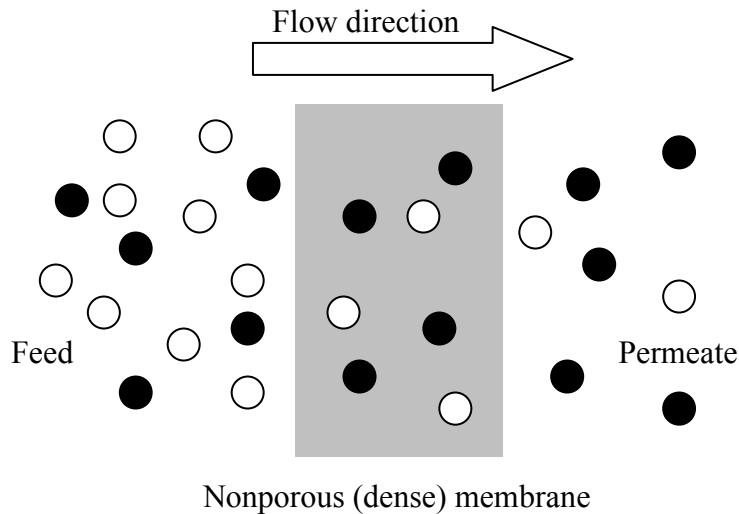


Fig. 1-9. Schematic of molecules transporting through a nonporous (dense) membrane

The transport mechanism can be described by a solution-diffusion model [Wijmans et al., 1995]. Permeability can be written:

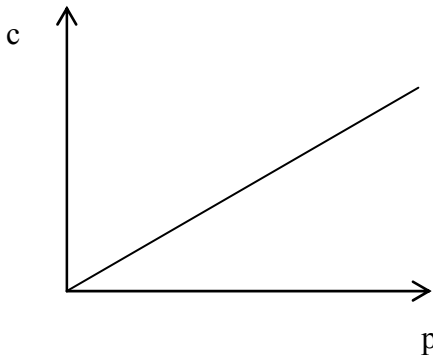
$$P = D \times S$$

where P is permeability coefficient, D is diffusion coefficient, and S is solubility. In this model, first, penetrants dissolve into the membrane and then they diffuse through the membrane. Separation is achieved by differences in the amount of penetrants that dissolves in the membrane (i.e., solubility) and the rate at which the penetrants diffuse through the membrane (i.e., diffusivity).

The solubility of gases in elastomers is generally very low and can be described by Henry's law [Mulder, 1996]. Henry's law describes a linear relationship between the concentration of gases in polymer (c) and the penetrant pressure (p). It can be written as follows:

$$c = k_D \times p$$

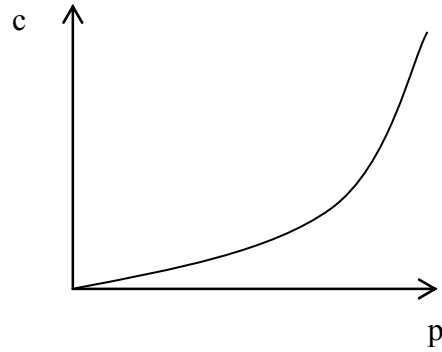
The proportionality constant, k_D , is referred to as the Henry's law constant. The plot of this relationship is shown in Fig. 1-10a which is called a sorption isotherm. In this case, where the solubility is very low, the diffusion coefficient can be considered constant. For small non-interacting molecules, the diffusion coefficient decreases as the molecular size increases. This system can be called an ideal system, where the solubility and the diffusion coefficient are independent of penetrant concentration.



Henry's law; linear
Gases in elastomers

Fig. 1-10a. Sorption isotherm for gases in elastomers

On the other hand, when the penetrants are organic vapors/liquids, the situation is different. Henry's law is not obeyed and a non-linearity is seen at high pressures (Fig. 1-10b).



Highly non-linear at high pressures

Organic vapor/liquids in polymers

Fig. 1-10b. Sorption isotherm for organic vapor/liquids in polymers

The solubility will be high and the diffusion coefficient will be concentration-dependent. This system can be called a non-ideal system, where the solubility and the diffusion coefficient are concentration-dependent. Therefore, two systems should be considered separately: an ideal system where the solubility and the diffusivity coefficient are constants, and non-ideal system where the two measures are concentration-dependent.

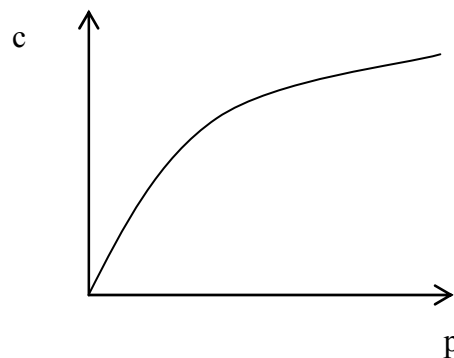
For glassy polymers, linearity deviates at high pressures (Fig.1-10c). Dual-mode model can be employed to explain this curvature. The theory assumes that there are two types of sorption modes: Henry's law sorption and Langmuir type sorption as well as two types of diffusion modes [Hu et al., 2003]. The schematic of the sorption isotherm for each sorption type is shown in Fig. 1-11. Concentration of penetrants in polymer is the addition of the two concentrations:

$$c = c_D + c_H$$

where c_D is the concentration of the penetrant sorbed onto the polymer by Henry's law sorption and c_H is the concentration of the penetrant sorbed onto the polymer by Langmuir type sorption. Equation becomes:

$$c = k_D p + \frac{c'_H b p}{1 + b p}$$

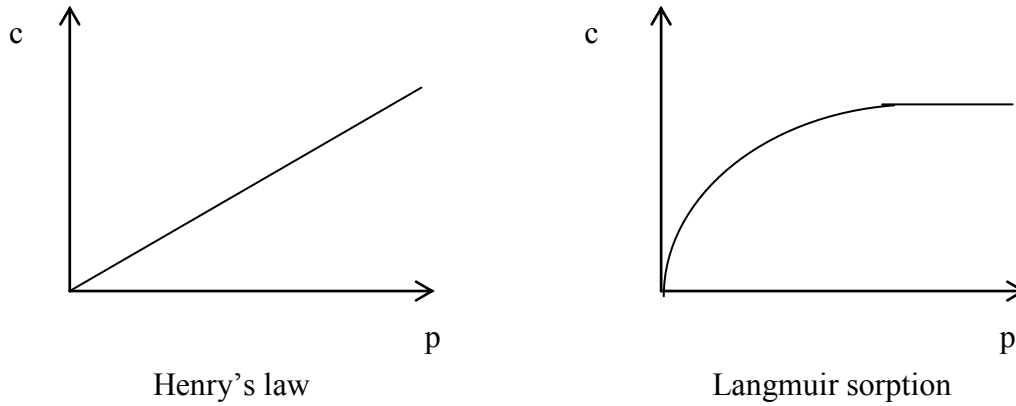
where k_D is the Henry's law constant, p the system pressure, c'_H the saturation constant and b the hole affinity constant.



Non-linear

Gases in glassy polymers

Fig. 1-10c. Sorption isotherm for gases in glassy polymers



Dual sorption theory

Fig. 1-11. Schematic of the sorption isotherm for the dual sorption theory

The driving force for transport can be pressure, temperature, concentration, and electromotive force [Wijmans, 1995]. These can all be written in terms of chemical potential gradient. Flux, J , through a plane perpendicular to the direction of diffusion can be expressed as:

$$J = -L \frac{d\mu}{dx}$$

where μ is the chemical potential, x the position within the membrane and L a proportionality coefficient. Hence, $d\mu/dx$ demonstrates the chemical potential gradient in the direction of diffusion. If the driving forces were to be expressed as concentration and pressure gradients, chemical potential will be written as:

$$d\mu = RTd \ln(\gamma \cdot c) + v dp$$

where c is the molar concentration of the penetrant, γ the activity coefficient, and v the molar volume of the penetrant.

The solution-diffusion model assumes that the pressure within a membrane is uniform and that the chemical potential gradient across the membrane is expressed only as a concentration gradient, without the pressure gradient. Hence,

$$J = -\frac{RTL}{c} \frac{dc}{dx}$$

Replacing RTL/c with the diffusion coefficient D , the equation becomes the Fick's first law.

$$J = -D \frac{dc}{dx}$$

To further discuss transport through a nonporous membrane using this Fick's law, concentration-independent system (ideal system) and concentration-dependent system (non-ideal) should be discussed separately [Mulder, 1996].

Transport in ideal systems

Here, ideal systems where solubility and diffusion coefficient are independent of the concentration are discussed [Mulder, 1996]. In these cases, the penetrants are small non-interacting gases such as helium, hydrogen, argon, nitrogen, oxygen and methane. The solubility of these gases in polymers can be described by Henry's law. As explained earlier, Henry's law depicts the linear relationship between the concentration of the penetrant in the polymer (c) and the pressure of the system (p). Henry's law is written as follows:

$$c = S \times p$$

c is the concentration of the gases in the polymer, S the solubility coefficient, p the pressure of the system. Substituting this equation into Fick's law, $J = -Ddc/dx$,

$$J = -DS \frac{dp}{dx}$$

Integrating this equation across the membrane, for which $x = 0$ and $p = p_1$ represent the position and pressure of the feed side respectively and $x = L$ and $p = p_2$ represent the position and pressure of the permeate side respectively, will give the following:

$$J = \frac{DS}{L}(p_1 - p_2)$$

Since $P = D \times S$,

$$J = \frac{P}{L}(p_1 - p_2)$$

This equation shows the relationship between the flux, J , and the permeability, P . According to this equation, the flux is proportional to the pressure difference across the membrane ($p_1 - p_2$) and inversely proportional to the membrane thickness, L .

As permeability depends on solubility and diffusivity, we will further look into these two measures for ideal systems. The diffusion coefficient increases as the size of the gas molecules decreases. This can be explained by an equation that shows that the frictional resistance of a molecule (f) increases as the radius of the molecule (r) increases and another equation that shows that the diffusion coefficient is inversely proportional to the frictional resistance [Mulder, 1996].

$$f = 6\pi\eta r$$

$$D = \frac{kT}{f}$$

Hence,

$$D = \frac{kT}{6\pi\eta r}$$

Therefore, it can be said that the diffusion coefficient decreases as the size of the gas molecules (i.e., r) increases.

On the other hand, solubility increases as the size of gas molecules increases. The reason for this is as follows. Since dissolution of penetrants into polymers can be considered as two steps: penetrant condensation and penetrant mixing with the polymer matrix, solubility highly relates with condensability of the penetrant molecules. Solubility increases as condensability increases. Condensability increases as the molecular size increases so large organic vapors/liquids have a higher condensability than small non-interacting gas molecules. Therefore, it can be said that the solubility increases as molecular size increases. Table 1-2 shows the critical temperature, T_c , and the solubility coefficient S of different gases in natural rubber [Brown et al., 1970]. T_c is a measure of condensability, i.e. the higher the T_c , the more condensable the substance. It demonstrates that as T_c increases, the solubility increases.

Table 1-2. Critical temperature and solubility of gases in natural rubber (Brown et al., 1970)

Gas	T_c [K]	S [$\text{cm}^3/(\text{cm}^3 \text{ cmHg})$]
H ₂	33.3	0.0005
N ₂	126.1	0.0010
O ₂	154.4	0.0015
CH ₄	190.7	0.0035
CO ₂	304.2	0.0120

Permeability can also depend on temperature, arising both from the dependence of diffusivity and solubility. The temperature dependence of the permeability coefficient can be written:

$$P = P_0 \exp\left(-\frac{E_p}{RT}\right)$$

E_p is the activation energy for permeation and P_0 a temperature independent constant.

The temperature dependence of the solubility of small non-interactive gases in polymers can be written:

$$S = S_0 \exp\left(-\frac{\Delta H_s}{RT}\right)$$

ΔH_s is the heat of solution and S_0 is the temperature-independent constant. Dissolution of a penetrant into a polymer takes two steps: penetrant condensation and penetrant mixing with the polymer matrix. Hence, the heat of solution, ΔH_s , contains both the heat of condensation, $\Delta H_{\text{condensation}}$, and the heat of mixing, ΔH_{mixing} .

$$\Delta H_s = \Delta H_{\text{condensation}} + \Delta H_{\text{mixing}}$$

If ΔH_s is negative, the process is exothermic and if it is positive, the process is endothermic. $\Delta H_{\text{condensation}}$ is always negative, which indicates a exothermic process, where heat is released when condensation occurs and increases in magnitude as penetrant condensability increases. For small non-interactive gases, the heat of solution has a small positive value which indicates endothermic process and the solubility increases slightly with increasing temperature.

The temperature dependence of the diffusivity of small non-interactive gases in polymers can be written:

$$D = D_0 \exp\left(-\frac{E_d}{RT}\right)$$

where E_d is the activation energy for diffusion and D_0 a temperature-independent constant.

$$P = D_0 S_0 \exp\left(-\frac{\Delta H_s + E_d}{RT}\right) = P_0 \exp\left(-\frac{E_p}{RT}\right)$$

For small non-interactive gases, the temperature effect of the permeability coefficient depends on diffusion rather than solubility since the solubility is small and hence, its temperature dependence is small.

Transport in non-ideal systems

Here, non-ideal systems where solubility and diffusion coefficient are dependent on concentration are discussed [Mulder, 1996]. In these cases, the penetrants are interacting gases such as large gas molecules or organic vapors. As solubility increases with large molecules, the heat of sorption is negative, which indicates an exothermic process and the solubility decreases as temperature increases. On the other hand, diffusivity is dependent on penetrant concentration and therefore is hard to discuss compared to the ideal system. An example of a non-ideal system may be carbon dioxide permeating through a polymer, especially high free volume polymer. Carbon dioxide is considered to plasticize glassy polymers at high pressures. At high pressures, carbon dioxide acts as an agent to swell the polymer and hence, affect the permeability of the

polymer. When the pressure reaches what is called a plasticization pressure, the permeability starts increasing as the feed pressure is increased. There are researches done to learn the mechanism of this plasticization effect [Bos et al., 1999].

Permeability

Permeability depends on factors such as sample history (the conditions that the polymer membrane encountered during formation) and the test conditions (temperature, pressure, and penetrant) [Mulder, 1996]. Penetrants such as helium, hydrogen, nitrogen, argon and oxygen are non-interacting gases, whereas gases such as carbon dioxide, sulfur dioxide, hydrogen sulfide, ethylene, propylene are interacting gases. Two structural parameters that affect the permeability are: glass transition temperature (T_g) and crystallinity. Glass transition temperature determines whether the polymer is glassy or rubbery whereas crystallinity determines whether the polymer is (semi-) crystalline or amorphous. Transport occurs mainly through the amorphous portions, so it is understandable that the degree of crystallinity affects the permeability.

To measure the permeability of a gas through the membrane, there are two available methods. First one is the constant pressure/variable volume method as shown in Fig. 1-12a. In this method, the feed side will be pressurized with the penetrant gas at a constant pressure. Gas permeation flux will be measured by a mass flowmeter or a soap film flowmeter.

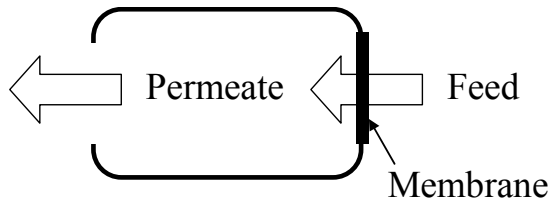


Fig. 1-12a. Schematic of constant pressure/variable volume method

The second method shown in Fig. 1-12b utilizes an apparatus that has a fixed volume on the permeate side which is pressurized by the penetrant that permeated through the membrane. This method is termed as constant volume/variable pressure method. The rate of increase in pressure on the permeate side will be monitored by a pressure transducer or a pressure gauge.

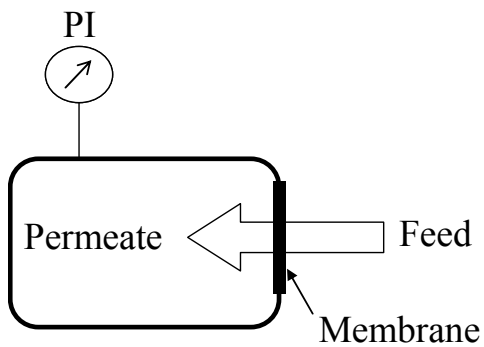


Fig. 1-12b. Schematic of constant volume/variable pressure method

Membrane Technology with Supercritical Fluids

There are several researches that have combined the two technologies: supercritical fluid processing and membrane technology. Semenova et al. [1992] conducted separation between supercritical CO₂ and ethanol using an asymmetric polyimide membrane in the purpose of recovering ethanol. Also with the asymmetric polyimide membrane, Higashijima et al. [1994] performed separation between supercritical CO₂ and petroleum components for enhanced oil recovery. In both of these researches, the major component of the retentate stream was supercritical CO₂. In comparison, several studies are done where supercritical CO₂ was the permeate and the solute was the retentate. In these researches, apparatus was designed which contained an extraction column followed by a membrane set-up. Spricigo et al. [2001] have reported on the separation of nutmeg essential oil and dense CO₂ using a cellulose acetate membrane. High retention factor of nutmeg essential oil and high CO₂ flux were obtained in their experiments. Tan et al. [2003] designed an apparatus where the extraction column was followed by a membrane set-up. Separation of caffeine and supercritical CO₂ was performed by means of a nanofilter M5 hollow membrane (Tech-Sep Co.), which consists of a thin layer of ZrO₂-TiO₂ coated on a carbon substrate. The inorganic layer had an average pore size of 3 nm. When the transmembrane pressure was kept constant at 0.2 MPa and temperature at 308 K, they obtained caffeine rejection of 100% and the highest CO₂ permeation flux at the feed pressure of 7.95 MPa. Peinemann et al. [2004] developed a method using a composite membrane of polyether imide being the porous support membrane and Teflon AF 2400 being the nonporous selective membrane in order to separate tocopherolacetate from supercritical CO₂. Teflon AFs are licensed products of

DuPont, which are amorphous, glassy copolymers consisting of 2,2-bis(trifluoromethyl)-4,5-difluoro-1,3-dioxole (PDD) and tetrafluoroethylene (TFE) [Buck et al., 1993]. Carlson et al. [2005] investigated separation of D-limonene from supercritical CO₂ using reverse osmosis membranes. They observed that 70% of the CO₂ can be recycled with the need of only small amount of pressurization, which would contribute greatly to the reduction of recompression cost.

Work in This Thesis

In this work, use of a nonporous polymer membrane was proposed to raise the particle collection yield in SAS process. The membrane would be placed at the outlet of the precipitation cell so as to let supercritical CO₂ and solvent permeate through the membrane and retaining the particles in the retentate (Fig.1-13).

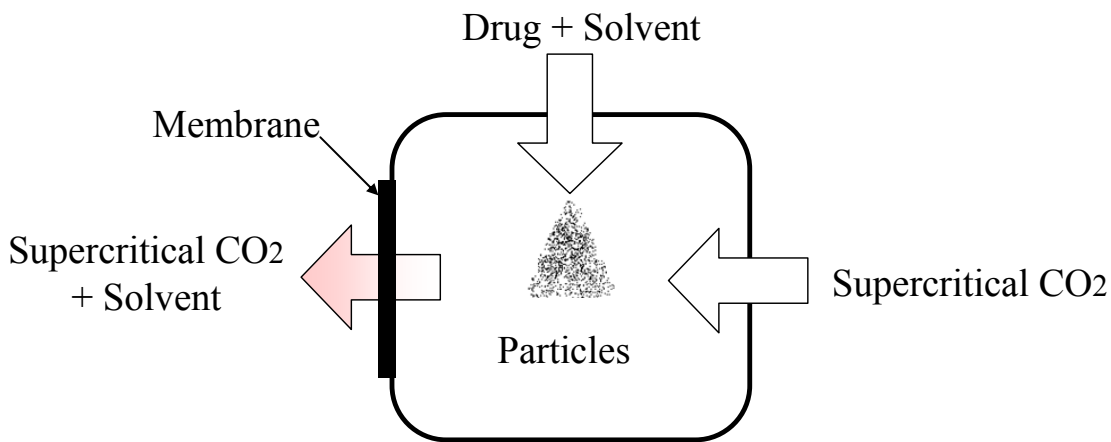


Fig. 1-13. Schematic of a supercritical antisolvent (SAS) process with membrane separation

Therefore, as a first step, permeation tests of CO₂ through Teflon AF products were conducted. Teflon AF was selected due to its high gas and solvent permeability as well as

its chemical and thermal inertness. In addition, its nonporosity is favored in this situation to prevent particle clogs to occur and to make this process viable for any range of particle size. The gas/vapor permeability property of this copolymer has been investigated earlier by several researchers, but most of the work has been performed at low pressures [Pinnau et al., 1996; Alentiev et al., 1997; Merkel et al., 1999; Polyakov et al., 2003]. In this work, CO₂ permeability data was obtained at higher pressures and compared with the data acquired for semicrystalline polytetrafluoroethylene (PTFE). As a second step, the permeability of an organic solvent with CO₂ was measured. Acetone was chosen as the organic solvent. Lastly, the permeability of drug particles in organic solvent was investigated. Tetracycline was chosen as the drug particles and methanol as the solvent to dissolve the drug.

CHAPTER 2

AMORPHOUS TEFLON MEMBRANE

Teflon AF products (DuPont, Wilmington, DE) are amorphous, glassy random copolymers consisting of 2,2-bistrifluoromethyl-4,5-difluoro-1,3-dioxole (PDD) and tetrafluoroethylene (TFE). The chemical structure of this copolymer is shown in Fig. 2-1.

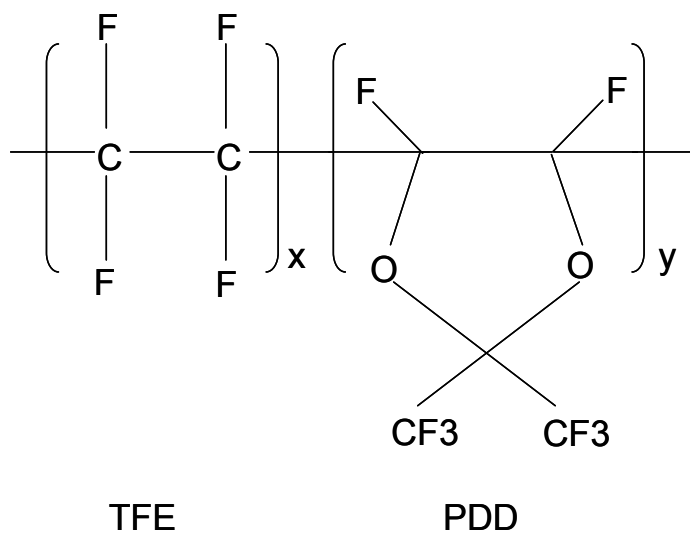


Fig. 2-1. Chemical structure of Teflon AF product: amorphous, glassy random copolymer of 2,2-bistrifluoromethyl-4,5-difluoro-1,3-dioxole (PDD) and tetrafluoroethylene (TFE). $x = 13$ mol %, $y = 87$ mol % for Teflon AF 2400 and $x = 35$ mol %, $y = 65$ mol % for Teflon AF 1600

Teflon AF 2400 contains 87 mol% PDD and 13 mol% TFE with the transition temperature of 240 °C, whereas Teflon AF 1600 contains 65 mol% PDD and 35 mol% TFE with $T_g = 160$ °C. Teflon AFs have high temperature stability and chemical resistance, as well as high free volume compared to other glassy polymers [Buck, 1993]. It is a nonporous (dense) membrane as shown in the micrograph taken by a scanning electron microscope (SEM) (Fig. 2-2). The micrograph on the right shows the edge of a film which has a thickness of approximately 60 μm . The micrograph on the left is at higher magnification and there were no pores seen.

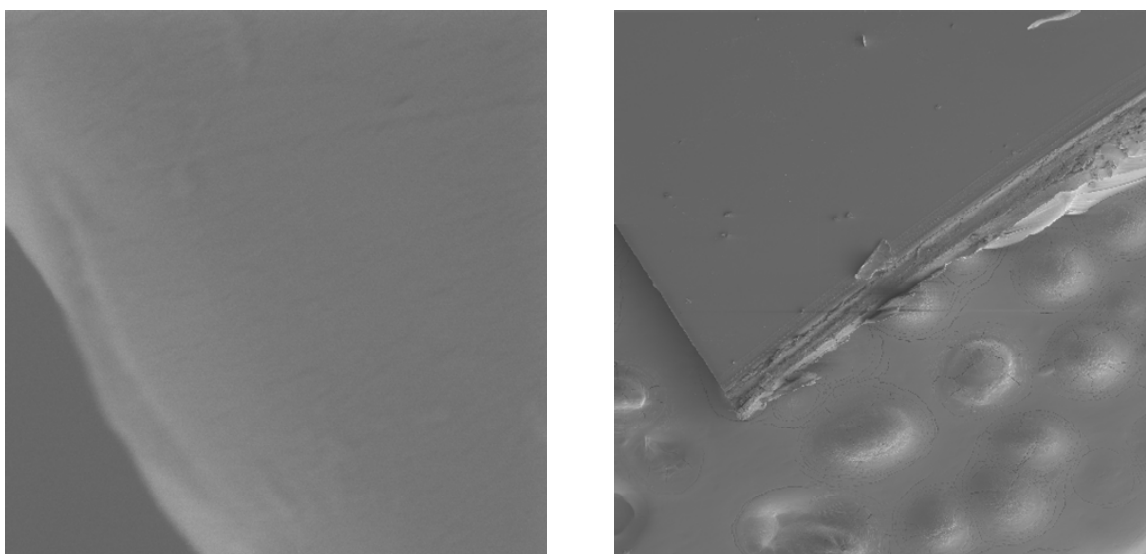


Fig. 2-2. Micrograph of a Teflon AF 2400 film taken by a scanning electron microscope

In Teflon AF, the side chains on the dioxole contribute to its high free volume. Free volume can be quantified by a measure called fractional free volume, FFV:

$$\text{FFV} = \frac{V - V_0}{V}$$

where V is the molar volume and V_0 the volume occupied by the polymer chains. V can be calculated by dividing the MW of the polymer by the density which can be determined experimentally.

$$V = \frac{MW}{\rho}$$

V_0 can be calculated using Bondi [1968]'s approximation which is as follows:

$$V_0 = 1.3 \times V_w$$

where V_w is the van der Waals volume. V_w can be calculated using a group contribution method [Krevelen, 1990]. The values of FFV for Teflon AF 2400 obtained by Pinnau et al. [1996] was 0.327 respectively. This value is in the same range as that of poly(1-trimethylsilyl-1-propyne) (PTMSP) which was measured as 0.34 by Alentiev et al. [1997], but higher than those of other glassy polymers which are typically in the range of 0.14-0.23 [Bos et al., 1999].

The permeability property of this copolymer has been investigated earlier by several researchers, but most of the work has been performed mainly at low pressures [Pinnau et al., 1996; Alentiev et al., 1997; Merkel et al., 1999; Polyakov et al., 2003].

Pinnau et al. [1996] have made Teflon AF 2400 film from solvent-cast method and obtained films with thickness of 14-20 μm . The permeation measurements were tested with a membrane of surface area of 12.6 cm^2 by a constant pressure/variable volume method. Pure gas permeation measurements were performed at 25-60 $^\circ\text{C}$ and a pressure difference of 20-120 psig across the membrane (atmospheric pressure at the permeate side). Gas flow rates were monitored by a soap film flowmeter. The calculation was done by the following equations:

$$J = \frac{273}{TA} \frac{P_{\text{atm}}}{76} \left(\frac{dV}{dt} \right)$$

$$P = \frac{J \cdot L}{p_2 - p_1}$$

where J is the permeation flux, P_{atm} the atmospheric pressure, A the membrane surface area, T the absolute temperature, and dV/dt the volumetric flow rate monitored by the soap film flowmeter. P is the permeability coefficient, p_2 the feed/retentate (upstream) pressure, p_1 the permeate (downstream) pressure (atmospheric), and L the membrane thickness. Gas mixture permeation measurements were performed at 25 °C and a pressure difference of 200 psig. The compositions of the retentate and the permeate were analyzed by a gas chromatograph with a TCD detector. They observed that Teflon AF 2400 showed a higher permeability than other glassy polymers, although less than that of poly 1-trimethylsilyl-1-propyne (PTMSP). Teflon AF 2400 showed higher permeability for small gas molecules than large, condensable gases. This indicates that the diffusion coefficient is high for the small gas molecules, resulting in high permeability. On the other hand, PTMSP showed higher permeability for large, condensable gases than small gas molecules. This indicates that PTMSP exhibits higher permeability mainly due to high solubility whereas Teflon AF 2400 exhibits high permeability mainly due to high diffusion coefficient. The temperature dependence of the gas permeability of Teflon AF 2400 was very weak. The vapor permeability of Teflon AF 2400 increased greatly with the vapor activity, indicating plasticization of the polymer.

Alentiev et al. [1997] made Teflon AF 2400 and Teflon AF 1600 film using solvent-cast method in which the films were cast from 2 wt % of perfluorotoluene solutions. For Teflon AF 2400, the solvent was evaporated at 55 °C whereas for Teflon

AF 1600, the solvent was evaporated at ambient temperature. Then, the films were dried in vacuum at 40-50 °C. Permeability and diffusion coefficient were measured by a mass spectrometric method for different gases such as He, H₂, O₂, N₂, CO₂, and hydrocarbons C₁-C₃. The measurements were conducted at 22 °C with pressure difference of 0.0013-0.027 MPa across the membrane (vacuum on the permeate side). They found that high permeability was exhibited especially for lighter gases, i.e. He and H₂. No dependence of permeability on feed pressure was seen. A value of 2600 barrer was obtained for CO₂ permeability. Also, they have estimated and measured the free volume of the perfluorodioxole copolymers by Bondi's method [Krevelen, 1990] and positron annihilation lifetime (PAL) method respectively.

Merkel et al. [1999] have made Teflon AF 2400 film from solvent-cast method and obtained films with thickness of 50 µm. The permeation measurements were tested with a membrane of surface area of 13.8 cm² by a constant pressure/variable volume method. Pure gas permeation measurements were performed at 25-60 °C and a pressure difference of 15-240 psig across the membrane (atmospheric at the permeate side). The calculation was done in the same way as Pinnau et al. [1996]. They obtained the CO₂ permeability value of 2200 barrer at 35 °C. They have compared the permeability of Teflon AF 2400 with that of PTMSP and polysulfone (PSF). The value for Teflon AF 2400 fell between the two: larger than that of PSF and smaller than that of PTMSP. PSF is a size-sieving, low free volume glassy polymer whereas PTMSP is a weakly size-sieving, high free volume glassy hydrocarbon-rich polymer. Since size-sieving character is affected by the polymer's diffusion coefficient, it can be said that the diffusion coefficient of Teflon AF 2400 affects its permeability to a larger extent compared to

PTMSP and to a smaller extent compared to PSF. This is similar to observation of Pinnau et al. [1996], where it was shown that the high diffusion coefficient of Teflon AF 2400 largely contributed to its high permeability.

Table 2-1 shows the CO₂ permeability through various polymer membranes studied by researchers previously.

Table 2-1. CO₂ permeability coefficients in different polymers studied previously

Polymer	P [barrer]	T [°C]	p_f [psig]	Δp (psi)	Reference
PTMSP	30000	25	50	50	I. Pinnau, 1993
Polycarbonate	8	25	50	50	H. J. Bixler, 1971
PTFE	12				S. M. Nemser, 1991
Matrimid 5218	34	50	1465.5	1465.5	S. Damle, 2003
PDMS	3200	40			I. Blume
Polysulfone	5-8	35	14.7-132.3		C. Hu, 2003
IPC	3016-6032	40	1217.8	43.5	V. E. Patil, 2006
PVA	2180-4360	40	1130.8	43.5	V. E. Patil, 2006

PTMSP : poly1-trimethylsilyl-1-propyne

PTFE : polytetrafluoroethylene

Matrimid 5218 : commercial polyimide

PDMS : polydimethylsiloxane

IPC : polyamide copolymer

PVA : polyvinyl alcohol

Table 2-2 shows the CO₂ permeability through Teflon AF 2400. The differences in the permeability coefficient values are considered to be coming from the differences in the condition at which the films were formed.

Table 2-2. CO₂ Permeability coefficients in Teflon AF 2400 studied previously

Reference	P [barrer]	T [°C]	p_f [MPa]	Δp [MPa]
S. M. Nemser, 1991	2800	25	1.7	1.6
I. Pinnau, 1996	3900	25	0.45	0.35
A. Y. Alentiev, 1997	2600	22	0.013-0.037	0.013-0.037
T. C. Merkel, 1999	2200	35		0

S. M. Nemser, 1991 : melt-pressed

I. Pinnau, 1996 : solvent cast from perfluoro-N-methyl morpholine (PF 5052), air-dried overnight at ambient condition, dried in a vacuum oven at 150 °C for 3 days

A. Y. Alentiev, 1997 : cast from perfluorotoluene, dried at 55 °C, dried in a vacuum oven at 40-50 °C

T. C. Merkel, 1999 : cast from PF 5060, dried at ambient condition

CHAPTER 3

EXPERIMENTAL METHODS

Polytetrafluoroethylene (PTFE) film was purchased from Small Parts, Inc., Miami Lakes, FL. It has a high crystallinity and a high melting temperature. Teflon AF 2400 and Teflon AF 1600 films of thickness ranging from 40-60 μm were obtained from Random Technologies, San Francisco, CA, under license from DuPont (reference 040225-0004 and 060221-0001). AF 2400 is a copolymer of 87 mol% 2,2-bis(trifluoromethyl)-4,5-difluoro-1,3-dioxole (PDD) and 13 mol% tetrafluoroethylene (TFE), having a glass transition temperature of 240 °C. AF 1600 is a copolymer consisting of 65 mol% PDD and 35 mol% TFE, having a T_g of 160 °C. These copolymers have a high free volume compared to other glassy polymers. Carbon dioxide used in the experiments had a purity of 99.9999% purchased from Airgas South, Inc., Atlanta, GA.

(1-a) Membrane set-up for CO₂ permeation test using constant volume method

The schematic of the membrane set-up is shown in Fig.3-1. CO₂ was pressurized by a syringe pump (Model 500D, Teledyne ISCO, Lincoln, NE) and feed pressure was measured by a pressure gauge (High Pressure Equipment, Erie, PA) indicated PI 1 in Fig. 3-1. The polymer membrane film was set inside a stainless steel filter holder (model XX45 025 00, Millipore, Billerica, MA) between the Buna-N resin O-ring and the filter

support screen, and was sealed by hand with a hex wrench. The thickness of the membrane was measured with a micrometer before the placement into the holder. At high pressures, PTFE O-rings were inserted above and beneath the membrane to decrease the force put on the membrane surface due to tightening and to let the membrane have some space for expansion due to plasticization. A high-pressure vessel was attached to the permeate side of the filter holder so as to increase the permeate volume. Permeate pressure was measured by a pressure gauge (PI 2). The feed and the permeate side were bypassed by a valve to let gradual increase or decrease in pressure occur in the case of pressurization/depressurization. The system was maintained at a desired temperature by an Isotemp immersion circulator (Model 730, Fisher Scientific, Pittsburgh, PA) immersed in a water bath.

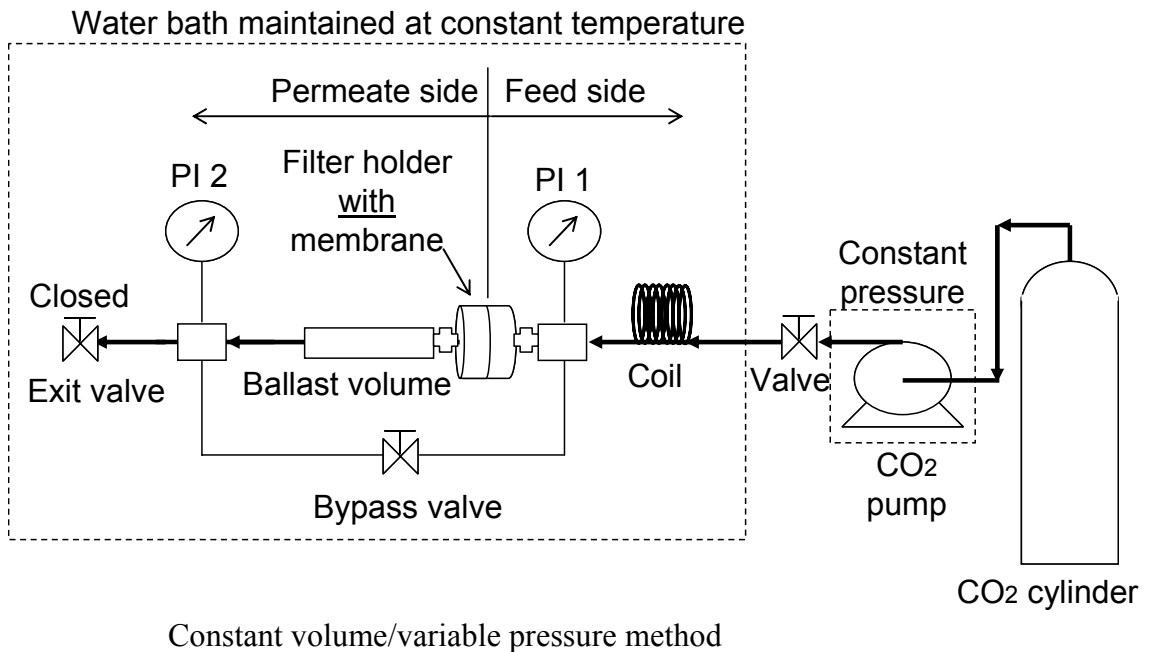


Fig. 3-1. Schematic of the membrane set-up for CO₂ permeation test

First, with the inlet valve and the bypass valve opened and the exit valve closed, the system was pressurized to the desired pressure. Then, the inlet and bypass valves were closed, and the pump was run at a pressure approximately 100 psi higher than the previous run. The experiment was initiated by opening the inlet valve and pressurizing the feed side to create pressure difference across the membrane, which will be the driving force for permeation. While the feed pressure was maintained constant by the pump, pressure increase in the constant permeate-side volume was recorded as a function of time. Permeation tests were performed up to the feed pressure of 1270 psig for Teflon AF 2400 and PTFE, and up to 630 psig for AF 1600. Permeability was given in the units of Barrer, which is equivalent to $10^{-10} \text{ cm}^3 \text{ (STP) cm} / (\text{s cm}^2 \text{ cmHg})$. The calculation of the permeability coefficient is described in the following section.

(1-b) Theory: CO₂ permeation test

The permeate flux in moles [$\text{mol} / (\text{s} \cdot \text{cm}^2)$] J can be calculated by:

$$J = \frac{1}{A} \frac{dn_p}{dt}$$

where n_p is the number of moles of penetrant (CO₂) on the permeate side and A is the area of the membrane [cm^2].

Permeability coefficient is defined as:

$$P = \frac{J \cdot L}{\Delta p}$$

where L is the membrane thickness [cm^2] and Δp is the pressure difference across the membrane [cmHg]. The permeability was calculated as follows:

$$p_p V_p = z n_p R T$$

Assuming z to be constant and taking derivatives on both sides,

$$\frac{dn_p}{dt} = \frac{V_p}{zRT} \frac{dp_p}{dt}$$

Hence, the molar flux, J , will be:

$$J = \frac{V_p}{zART} \frac{dp_p}{dt}$$

And the permeability coefficient, P , will be:

$$P = \frac{V_p L}{zART \Delta p} \frac{dp_p}{dt} \left[\frac{\text{mol} \cdot \text{cm}}{\text{s} \cdot \text{cm}^2 \cdot \text{cmHg}} \right]$$

Noting $\Delta P = p_f - p_p$ and arranging,

$$\begin{aligned} P &= - \frac{V_p L}{zART(p_f - p_p)} \frac{d(p_f - p_p)}{dt} \\ &= - \frac{V_p L}{zART} \frac{d \ln(p_f - p_p)}{dt} \end{aligned}$$

Changing the units from mol to cm^3 (STP),

$$P = - \frac{V_p L \cdot \text{MW}_{\text{CO}_2}}{zART \rho(\text{STP})} \frac{d \ln \Delta p}{dt} \left[\frac{\text{cm}^3(\text{STP}) \cdot \text{cm}}{\text{s} \cdot \text{cm}^2 \cdot \text{cmHg}} \right]$$

For the units of permeability of gases and vapors, barrer is frequently used:

$$1 \text{ barrer} = 10^{-10} \frac{\text{cm}^3(\text{STP}) \cdot \text{cm}}{\text{s} \cdot \text{cm}^2 \cdot \text{cmHg}}$$

From the above equation of P , it can be found that the slope, m , of the plot of $\ln \Delta p$ versus t ($d \ln \Delta p / dt$) is necessary to determine P . Fig. 3-2a shows the graph obtained from the CO_2 permeation experiment and the permeate pressure is plotted against time. In Fig.

3-2b, the plot of the logarithm of the pressure difference Δp versus t is shown. An equation fitted linearly to this plot can give the slope of this plot. And the permeability coefficient can be calculated.

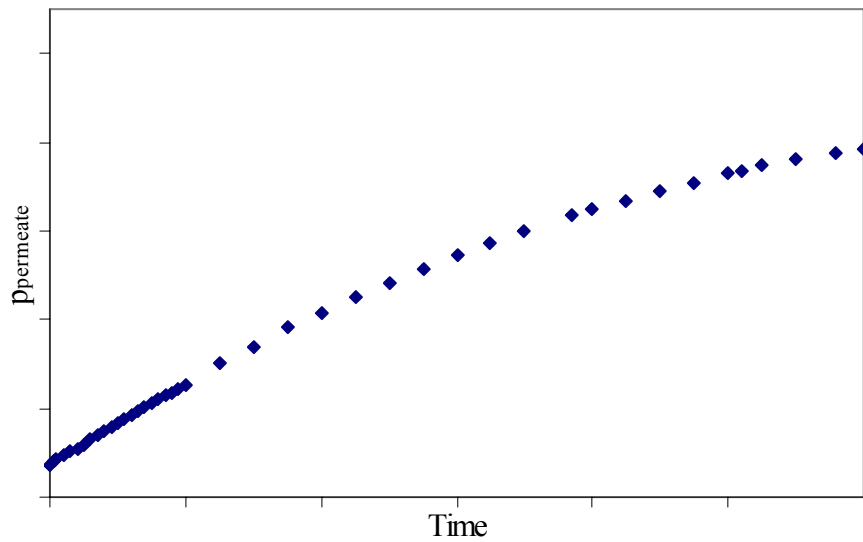


Fig. 3-2a. An example of a plot of permeate pressure vs time

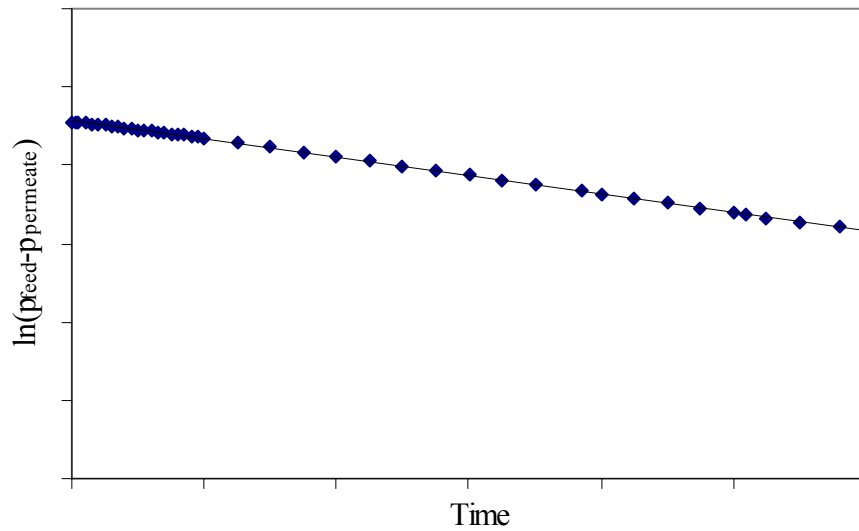


Fig. 3-2b. An example of a plot of logarithm of pressure difference vs time

(2-a) Set-up for verification of the system for acetone + CO₂ permeation

Material balance of the acetone was checked on the membrane set-up for the acetone + CO₂ permeation. This is to ensure that the calculation is done properly and that the data obtained is trustable. Also, it is useful for verifying that there is no leak in the system, although leaks were easily detectable by monitoring the system immersed in the water bath (If there were any leaks, air bubbles would have come out of the loose connections). This was done by analyzing the flow at the 6-port valve by a ultraviolet (UV)-visible (Vis) spectrophotometer (Genesys 2, Thermo Electron, Waltham, MA) and comparing the value obtained with the amount of acetone fed into the system. The schematic of the set-up is shown in Fig. 3-3.

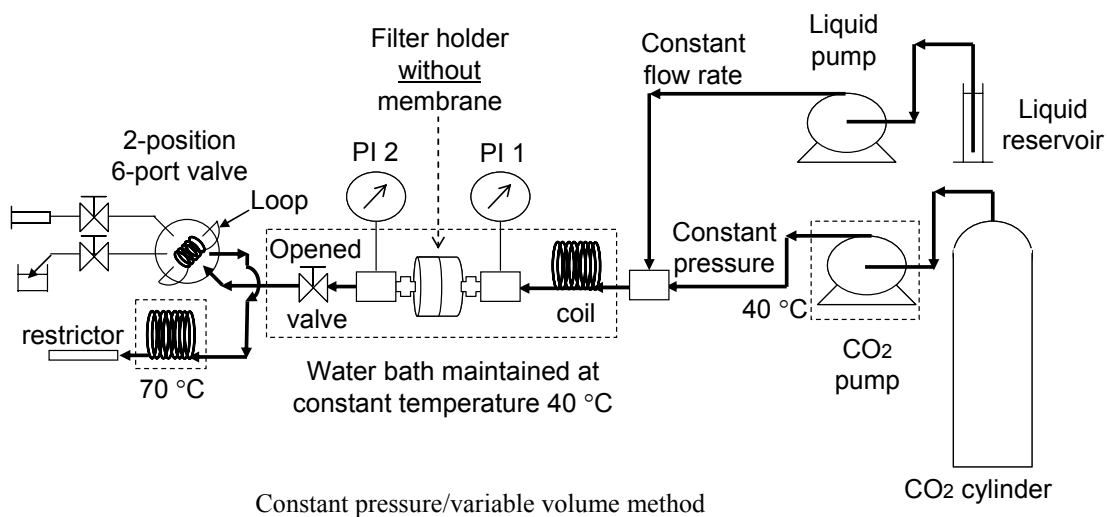


Fig. 3-3. Schematic of the set-up for verification of acetone + CO₂ permeation system

CO₂ was pumped by a syringe pump (Model 500D, Teledyne ISCO, Lincoln, NE) and acetone was pumped by a liquid pump (Scientific Systems, Inc. LabAlliance, State College, PA). The combined flow passed through a coil immersed in the water bath

maintained at 40 °C by an Isotemp immersion circulator (Model 730, Fisher Scientific, Pittsburgh, PA). The flow passed through the stainless steel filter holder (model XX45 025 00, Millipore, Billerica, MA) which did not have a membrane film inserted in between. System pressure was monitored by pressure gauges PI 1 and PI 2, both of which should have shown the same value due to absence of the membrane. After passing through a valve, the flow entered the 2-position 6-port valve (Model 7010, Rheodyne, Rohnert Park, CA) and exited to flow through the coil maintained at approximately 70 °C and finally flowed through a 75 µm polyetheretherketone-silica (PEEKsil) tubing which acted as a flow restrictor. The sampling was done at the 6-port valve when the loop of the valve was isolated from the rest of the system. The acetone collected in the isolated loop was slowly depressurized and washed with water to collect all of the acetone.

The experimental steps are as follows. The valve at the position after the filter holder was kept open throughout the experiment. CO₂ was continuously flowing in advance to acetone. It was run at constant pressure in the range of 8-10 MPa. After the CO₂ flow reached steady state, acetone flow was started at a constant flow rate ranging in 0.10-0.25 mL/min. Once enough time was given for the CO₂ and acetone flow to reach steady state, sampling was initiated at the 6-port valve by turning the valve to the position that would isolate the loop. The permeate stream contained in the loop was depressurized by opening the sampling valve and was collected in distilled water to absorb the acetone in the stream. Then, the loop was washed with distilled water to completely remove the acetone from the loop. After the sampling was complete, the 6-port valve was returned back to the position at which the loop was connected to the system again. The collected sample solution was analyzed by UV spectrophotometry to determine the acetone

concentration using the calibration curve made from known concentrations of acetone solutions. The absorption at 500 nm was recorded followed by the absorption at 266 nm. The calculation following this experiment is summarized in the following section.

(2-b) Theory: Verification of the system for acetone + CO₂ permeation

Amount of acetone collected at the 6-port valve was calculated from ultraviolet (UV) spectrophotometry analysis. For the solution collected, the absorption at 500 nm was first measured and then at 266 nm. The difference between these two values is considered the net absorption. From the calibration curve prepared with the solutions of known concentration, the concentration of the sample solution is calculated. Multiplying this concentration by the weight of the solution will give the amount of acetone in the solution.

To ensure that 100 % of the acetone fed into the system was maintained within the system, the amount of acetone experimentally collected (by UV) inside the loop of the 6-port valve will be compared with the amount of acetone that should be collected in the loop, which can be calculated from the amount of acetone fed into the system.

The amount of acetone that should be collected in the loop according to the amount of acetone fed into the system will be calculated as follows. First, the mole fraction of acetone in the acetone + CO₂ feed flow, $y_{\text{acetone, fed}}$, will be calculated. The mass flow rate of acetone fed, $m_{\text{acetone, fed}}$, was calculated from the volumetric flow rate of feed acetone at 27 °C, $v_{\text{acetone, fed}}^{27^\circ\text{C}}$:

$$m_{\text{acetone, fed}} = \rho_{\text{acetone}}^{27^\circ\text{C}} \cdot v_{\text{acetone, fed}}^{27^\circ\text{C}}$$

Next, the molar flow rate of acetone fed, $n_{\text{acetone, fed}}$, was calculated:

$$n_{\text{acetone, fed}} = \frac{m_{\text{acetone, fed}}}{\text{MW}_{\text{acetone}}}$$

The mass and molar flow rates of CO₂ will be calculated in the same way. The mass flow rate of CO₂ fed, $m_{\text{CO}_2, \text{ fed}}$, was calculated from the volumetric flow rate of CO₂ at 40 °C

and the system pressure p , $v_{\text{CO}_2, \text{ fed}}^{40^\circ\text{C}, p}$:

$$m_{\text{CO}_2, \text{ fed}} = \rho_{\text{CO}_2}^{40^\circ\text{C}, p} \cdot v_{\text{CO}_2, \text{ fed}}^{40^\circ\text{C}, p}$$

The molar flow rate of CO₂ fed, $n_{\text{CO}_2, \text{ fed}}$, was calculated:

$$n_{\text{CO}_2, \text{ fed}} = \frac{m_{\text{CO}_2, \text{ fed}}}{\text{MW}_{\text{CO}_2}}$$

Using the molar flow rates of acetone and CO₂, the molar fraction of acetone that was fed into the system can be calculated:

$$y_{\text{acetone, fed}} = \frac{n_{\text{acetone, fed}}}{n_{\text{acetone, fed}} + n_{\text{CO}_2, \text{ fed}}}$$

From pressure, p , temperature, T (40 °C), and acetone mole fraction in the acetone + CO₂ feed flow, $y_{\text{acetone, fed}}$, the compressibility factor, z , can be calculated using Peng-Robinson

Equation of State (PR-EOS), which is shown below.

$$p = \frac{RT}{V_m - b} - \frac{a\alpha}{V_m^2 + 2bV_m - b^2}$$

$$a = \frac{0.45724R^2T_c^2}{P_c}$$

$$b = \frac{0.07780RT_c}{P_c}$$

$$\alpha = \left(1 + \left(0.37464 + 1.54226\omega - 0.26992\omega^2\right)\left(1 - T_r^{0.5}\right)\right)^2$$

$$T_r = \frac{T}{T_c}$$

where V_m is the molar volume, T_c the critical temperature, P_c the critical pressure, R the gas constant, ω the acentric factor, T_r the reference temperature.

After obtaining z using the PR-EOS program, the molar volume of the acetone + CO_2 feed mixture, $v_{\text{mol,mixt}}$, can be calculated from the compressibility equation:

$$v_{\text{mol,mixt}} = \frac{zRT}{p}$$

Inverse of $v_{\text{mol,mixt}}$ is the molar density, $\rho_{\text{mol,mixt}}$:

$$\rho_{\text{mol,mixt}} = \frac{1}{v_{\text{mol,mixt}}}$$

The weight density, $\rho_{\text{g,mixt}}$, can be obtained by multiplying the molecular weight of the mixture, MW_{mixt} . First, the molecular weight of the mixture, MW_{mixt} , can be calculated as:

$$\text{MW}_{\text{mixt}} = (\text{MW}_{\text{acetone}})(y_{\text{acetone, fed}}) + (\text{MW}_{\text{CO}_2})(y_{\text{CO}_2, \text{ fed}})$$

Hence, the weight density of the mixture, $\rho_{\text{g,mixt}}$, can be calculated:

$$\rho_{\text{g,mixt}} = (\rho_{\text{mol,mixt}})(\text{MW}_{\text{mixt}})$$

If the assumption is made that the acetone fed was 100 % maintained within the system, from the weight density of the mixture, $\rho_{\text{g,mixt}}$, and the acetone mole fraction in the combined flow, $y_{\text{acetone, fed}}$, the weight of acetone that should be collected in the loop of the 6-port valve, $w_{\text{acetone_fed_loop}}$, can be calculated as:

$$W_{\text{acetone_fed_loop}} = \frac{(\rho_{\text{g,mixture}})(v_{\text{loop}})(y_{\text{acetone, fed}})(MW_{\text{acetone}})}{MW_{\text{mixt}}}$$

This acetone amount is the value that should be obtained at the loop of the 6-port valve, according to the amount of acetone fed into the system. This value, $w_{\text{acetone_fed_loop}}$, should be compared with the amount obtained from UV analysis, $w_{\text{acetone_UV_loop}}$. Percentage of the acetone collected in the loop of the 6-port valve is:

$$\text{Percentage} = \frac{W_{\text{acetone_UV_loop}}}{W_{\text{acetone_fed_loop}}} \times 100$$

(3-a) Membrane set-up for acetone + CO₂ permeation test

The schematic of the membrane set-up is shown in Fig. 3-4. CO₂ was fed by a syringe pump (Model 500D, Teledyne ISCO, Lincoln, NE) and acetone was pumped by a liquid pump (Scientific Systems, Inc. LabAlliance, State College, PA). CO₂ flow was diversified into two streams: one merging with the acetone flow and the other flowing to the permeate side of the membrane. This was done to keep the permeate pressure the same as the retentate pressure. The CO₂ flow that was combined with the acetone flow passed through a coil immersed in a water bath maintained at 40 °C by an Isotemp immersion circulator (Model 730, Fisher Scientific, Pittsburgh, PA).

The fluid inlet fitting was specially modified as shown in Fig. 3-4b so that there was enough space for 1/16" stainless steel tubings to go through and be set at positions near the membrane on both the feed/retentate and the permeate side. On the feed/retentate side, this modification allowed the acetone feed + CO₂ flow to pass through the outside

of the tubing and the retentate flow to pass through the inside of the tubing, which flowed to the retentate restrictor. On the permeate side, CO₂ flowed through the outside of the 1/16" stainless steel tubing and the permeate stream flowed through the inside of the tubing, which flowed to the 6-port valve. The feed/retentate pressure was measured by a pressure gauge (High Pressure Equipment, Erie, PA) indicated PI 1. The polymer membrane film was set inside a stainless steel filter holder (model XX45 025 00, Millipore, Billerica, MA) between the Buna-N resin O-ring and the filter support screen, and was sealed by hand with a hex wrench. The thickness of the membrane was measured with a micrometer before the placement into the holder. At high pressures, PTFE O-rings were inserted above and beneath the membrane to decrease the force put onto the membrane surface due to tightening and to let the membrane have some space for expansion due to plasticization. Permeate pressure was measured by a pressure gauge indicated PI 2. The permeate flow passed through a valve, then entered a 2-position 6-port valve (Model 7010, Rheodyne, Rohnert Park, CA), and flowed through the coil which was heated to approximately 70 °C in order to prevent CO₂ freezing at the outlet due to expansion. Finally, the stream flowed through a 75 µm polyetheretherketone-silica (PEEKsil) tubing which acted as a flow restrictor. CO₂ flow rate was measured by inverting a graduated cylinder in the water bath and collecting the flow that came out the restrictor during a certain amount of time. The system was maintained at 40 °C by an Isotemp immersion circulator (Model 730, Fisher Scientific, Pittsburgh, PA) immersed in a water bath. The sampling was done at the 6-port valve when the loop of the valve was isolated from the rest of the system. The acetone collected in the isolated loop was slowly depressurized into distilled water and washed additionally with water to collect all of the

acetone in the loop. The collected sample solution was analyzed by an ultraviolet-visible (UV-Vis) spectrophotometer (Genesys 2, Thermo Electron, Waltham, MA) to determine the acetone concentration from the calibration curve previously made.

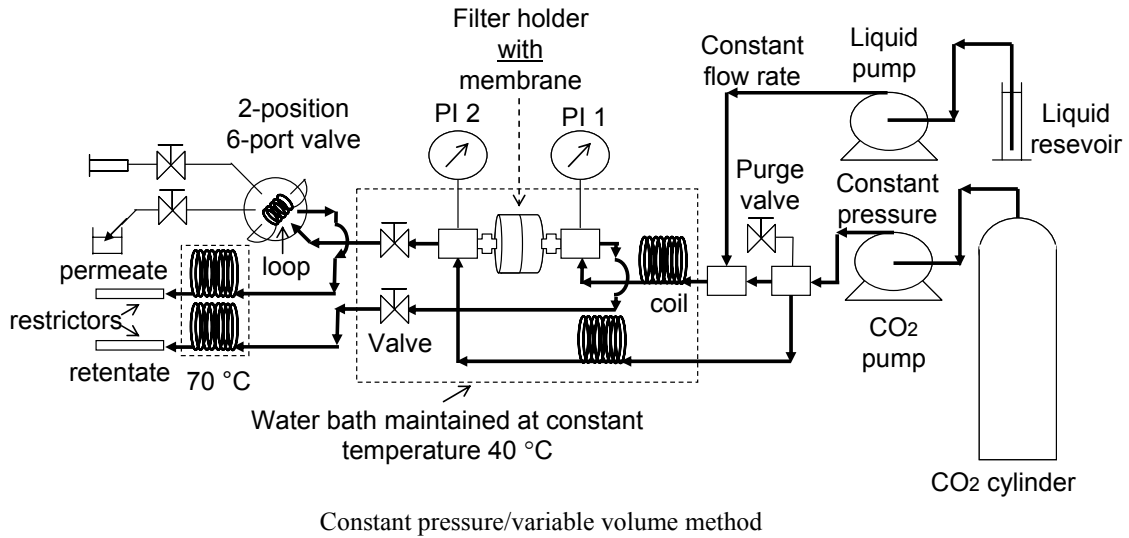


Fig. 3-4a. Schematic of the membrane-set up for acetone + CO₂ permeation

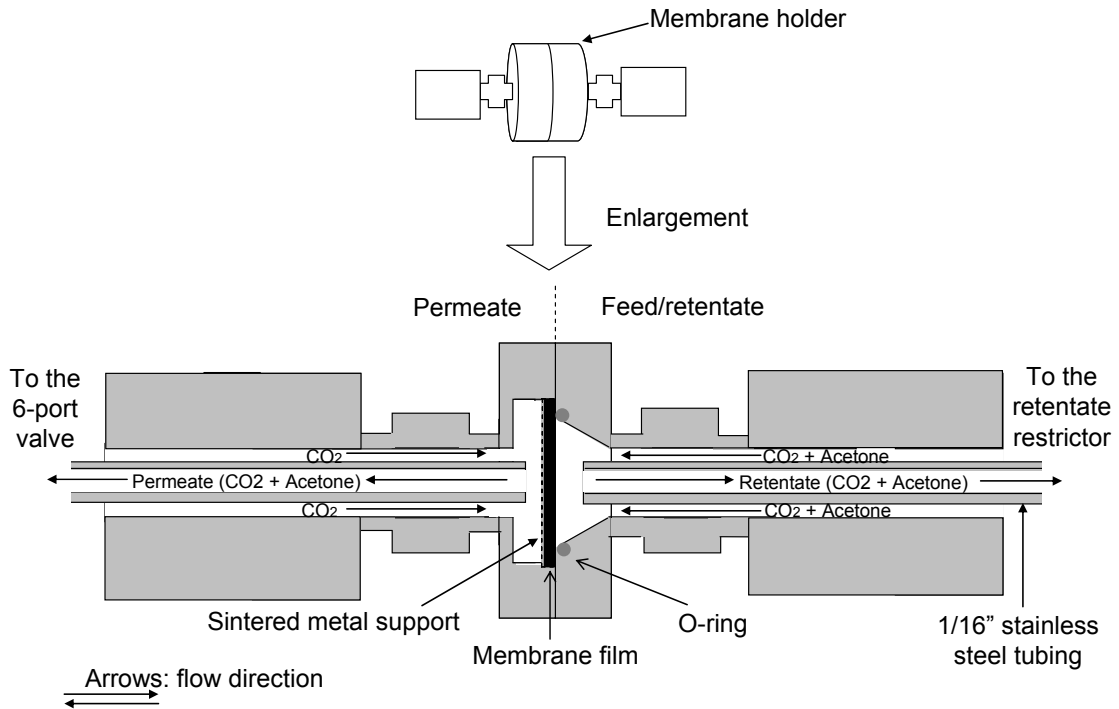


Fig. 3-4b. Enlargement of the schematic of the membrane holder

The experimental steps are as follows. The purge valve was kept closed, and the retentate and the permeate valve were kept open throughout the experiment. CO₂ was continuously flowed in advance to acetone and after reaching steady state, acetone flow was started at 0.50 mL/min. Once enough time was given for the CO₂ and acetone flow to reach steady state, sampling was initiated at the 6-port valve by turning the valve to the position that would isolate the loop. The permeate stream contained in the loop was depressurized by opening the sampling valve and was collected in distilled water to absorb the acetone in the stream. Then, the loop was washed with distilled water to completely remove the acetone from the loop. The collected sample solution was analyzed by UV spectrophotometry to determine the acetone concentration from the calibration curve previously made. The absorption at 500 nm was recorded followed by the absorption at 266 nm. The calculation following this experiment is summarized in the next section.

(3-b) Theory: CO₂ + acetone permeation test

Calculation of the percentage of acetone collected at the permeate side

The calculation for the CO₂ and acetone permeation test is the same as in the verification experiment for the set-up. Amount of acetone collected at the 6-port valve will be calculated from ultraviolet (UV) spectrophotometry analysis. For the solution collected, the absorption at 500 nm was first measured and then at 266 nm. The difference between these two values was considered as the net absorption. From the

calibration curve prepared beforehand with the solutions of known concentration, the concentration of the sample solution was calculated. Multiplying this concentration by the weight of the solution will give the amount of acetone in the solution.

To calculate what percentage of the feed permeated through the membrane, the amount of acetone collected inside the loop of the 6-port valve by UV analysis should be compared with the amount of acetone that will be collected in the loop when 100 % permeation was occurring, which can be calculated from the amount fed into the system. The latter value (amount of acetone that is to be collected in the loop when 100 % permeation occurs) will be calculated as follows. First, the mole fraction of acetone in the combined (acetone + CO₂) feed flow, $y_{\text{acetone, fed}}$, will be calculated from the volumetric flow rate of feed acetone at 25 °C, $v_{\text{acetone, fed}}^{25^\circ\text{C}}$, and the volumetric flow rate of feed CO₂ at 40 °C and 1 atm, $v_{\text{CO}_2, \text{ fed}}^{40^\circ\text{C}, 1\text{atm}}$:

$$y_{\text{acetone, fed}} = \frac{\frac{(\rho_{\text{acetone}}^{25^\circ\text{C}})(v_{\text{acetone, fed}}^{25^\circ\text{C}})}{\text{MW}_{\text{acetone}}}}{\frac{(\rho_{\text{acetone}}^{25^\circ\text{C}})(v_{\text{acetone, fed}}^{25^\circ\text{C}})}{\text{MW}_{\text{acetone}}} + \frac{(\rho_{\text{CO}_2}^{40^\circ\text{C}, 1\text{atm}})(v_{\text{CO}_2, \text{ fed}}^{40^\circ\text{C}, 1\text{atm}})}{\text{MW}_{\text{CO}_2}}}$$

From pressure, p , temperature, T , and acetone mole fraction in the feed, $y_{\text{acetone, fed}}$, the compressibility factor, z , can be calculated using Peng-Robinson Equation of State (PR-EOS).

After obtaining z using the PR-EOS program, the molar volume of the combined feed mixture, $v_{\text{mol, mixt}}$, can be calculated from the compressibility equation:

$$v_{\text{mol, mixt}} = \frac{zRT}{p}$$

Inverse of $v_{\text{mol,mixt}}$ is the molar density, $\rho_{\text{mol,mixt}}$:

$$\rho_{\text{mol,mixt}} = \frac{1}{v_{\text{mol,mixt}}}$$

The weight density, $\rho_{\text{g,mixt}}$, can be obtained by multiplying the molecular weight of the mixture, MW_{mixt} , with the molar density $\rho_{\text{mol,mixt}}$. First, the molecular weight of the feed mixture, MW_{mixt} , will be calculated:

$$MW_{\text{mixt}} = (MW_{\text{acetone}})(y_{\text{acetone, fed}}) + (MW_{\text{CO}_2})(y_{\text{CO}_2, \text{ fed}})$$

Hence, the weight density, $\rho_{\text{g,mixt}}$, can be calculated:

$$\rho_{\text{g,mixt}} = (\rho_{\text{mol,mixt}})(MW_{\text{mixt}})$$

If 100 % of the feed acetone permeated through the membrane, using the weight density of the mixture, $\rho_{\text{g,mixt}}$, and the acetone mole fraction in the combined feed flow, $y_{\text{acetone, fed}}$, the weight of feed acetone that will be collected in the loop, $w_{\text{acetone_fed_loop}}$, can be calculated:

$$w_{\text{acetone_fed_loop}} = \frac{(\rho_{\text{g,mixt}})(v_{\text{loop}})(y_{\text{acetone, fed}})(MW_{\text{acetone}})}{MW_{\text{mixt}}}$$

This acetone amount should be compared with the amount obtained from UV analysis.

Percentage of the acetone that permeated through the membrane is calculated:

$$\text{Percentage} = \frac{w_{\text{acetone_UV_loop}}}{w_{\text{acetone_fed_loop}}} \times 100$$

Calculation of the permeation flux and the permeability coefficient of acetone

The following will be the calculation of the permeation flux of acetone and the permeability coefficient of acetone. The CO₂ flow rate at the permeate and the retentate side was measured with inversed cylinder at the exit of the restrictors in the 40 °C water bath. Hence, the CO₂ flow rates measured were values at 40 °C and ambient pressure (1 atm). These volumetric flow rates can be converted into mass flow rate by multiplying the CO₂ density at that condition. The value of the density of CO₂ at the certain pressure and 40 °C was obtained from NIST webbook (webbook.nist.gov). The mass flow rate on the permeate and the retentate side of the membrane will be calculated:

$$m_{\text{CO}_2, \text{permeate}} = v_{\text{permeate}}^{40^\circ\text{C}, 1\text{atm}} \times \rho_{\text{CO}_2}^{40^\circ\text{C}, 1\text{atm}}$$

$$m_{\text{CO}_2, \text{retentate}} = v_{\text{retentate}}^{40^\circ\text{C}, 1\text{atm}} \times \rho_{\text{CO}_2}^{40^\circ\text{C}, 1\text{atm}}$$

Multiplying the CO₂ mass permeation rate, $m_{\text{CO}_2, \text{permeate}}$, with the CO₂ density at 40 °C and the system pressure, p , CO₂ volumetric flow rate can be obtained at the system condition:

$$v_{\text{CO}_2, \text{permeate}}^{40^\circ\text{C}, p} = m_{\text{CO}_2, \text{permeate}} \times \rho_{\text{CO}_2}^{40^\circ\text{C}, p}$$

From the UV analysis, the weight of acetone collected in the sample loop of the 6-port valve at the permeate side, $w_{\text{acetone_UV_loop}}$, was obtained. Dividing this value by the sample loop volume will give the concentration (w/v) of acetone in the acetone + CO₂ solution collected in the loop.

$$c_{\text{acetone, permeate}}^{40^\circ\text{C}, p} = \frac{w_{\text{acetone_UV_loop}}}{V_{\text{loop}}}$$

Assuming that the acetone exist only a sparing amount compared to CO₂, the CO₂ flow rate at the system condition, $v_{\text{CO}_2, \text{permeate}}^{40^\circ\text{C}, p}$, can be considered as the total (acetone + CO₂)

flow rate, $v_{\text{acetone}+\text{CO}_2,\text{permeate}}^{40^\circ\text{C},p}$. Multiplying the acetone concentration, $c_{\text{acetone,permeate}}^{40^\circ\text{C},p}$, with the total volumetric flow rate, $v_{\text{acetone}+\text{CO}_2,\text{permeate}}^{40^\circ\text{C},p}$, gives the mass flow rate of acetone that permeated through the membrane, $m_{\text{acetone,permeate}}$.

$$m_{\text{acetone,permeate}} = c_{\text{acetone,permeate}}^{40^\circ\text{C},p} \times v_{\text{acetone}+\text{CO}_2,\text{permeate}}^{40^\circ\text{C},p}$$

$$m_{\text{acetone,permeate}} = \frac{W_{\text{acetone_UV_loop}}}{V_{\text{loop}}} \times v_{\text{CO}_2,\text{permeate}}^{40^\circ\text{C},p}$$

The volumetric flow rate of acetone fed into the system at 25 °C, $v_{\text{acetone}}^{25^\circ\text{C}}$, can be converted to the mass flow rate of acetone, $m_{\text{acetone,feed}}$, by multiplying the acetone density at 25 °C, $\rho_{\text{acetone}}^{25^\circ\text{C}}$:

$$m_{\text{acetone,feed}} = v_{\text{acetone}}^{25^\circ\text{C}} \times \rho_{\text{acetone}}^{25^\circ\text{C}}$$

Hence, the mass flow rate of acetone that was retained within the retentate side, $m_{\text{acetone,retentate}}$, will be:

$$m_{\text{acetone,retentate}} = m_{\text{acetone,feed}} - m_{\text{acetone,permeate}}$$

Next, to calculate the partial pressures of acetone in the CO₂ + acetone flow on the permeate and the retentate side, the mass flow rate of acetone on each side ($m_{\text{acetone,permeate}}$, $m_{\text{acetone,retentate}}$) will be converted to molar flow rate by dividing the value by the molecular weight of acetone, MW_{acetone} .

$$n_{\text{acetone,permeate}} = \frac{m_{\text{acetone,permeate}}}{MW_{\text{acetone}}}$$

$$n_{\text{acetone,retentate}} = \frac{m_{\text{acetone,retentate}}}{MW_{\text{acetone}}}$$

The acetone mole fraction in the CO₂ + acetone flow on the permeate and the retentate side will be calculated:

$$y_{\text{acetone,permeate}} = \frac{n_{\text{acetone,permeate}}}{n_{\text{acetone,permeate}} + n_{\text{CO}_2,\text{permeate}}}$$

$$y_{\text{acetone,retentate}} = \frac{n_{\text{acetone,retentate}}}{n_{\text{acetone,retentate}} + n_{\text{CO}_2,\text{retentate}}}$$

The partial pressure of acetone in each side will be obtained by multiplying the system pressure with the acetone mole fractions, $y_{\text{acetone,permeate}}$ $y_{\text{acetone,retentate}}$.

$$P_{\text{acetone,permeate}} = P \times y_{\text{acetone,permeate}}$$

$$P_{\text{acetone,retentate}} = P \times y_{\text{acetone,retentate}}$$

Hence, the pressure difference of acetone across the membrane, $\Delta p_{\text{acetone}}$, can be calculated:

$$\Delta p_{\text{acetone}} = P_{\text{acetone,retentate}} - P_{\text{acetone,permeate}}$$

Defining J as the mass flux of acetone permeating through the membrane, the mass flow rate of acetone that permeated, $m_{\text{acetone,permeate}}$, should be divided by the membrane surface area A .

$$J_{\text{acetone,permeate}} = \frac{m_{\text{acetone,permeate}}}{A}$$

The acetone permeability, $P_{\text{acetone,permeate}}$, is calculated by multiplying the membrane thickness, L , and dividing by the acetone pressure difference across the membrane, $\Delta p_{\text{acetone}}$:

$$P_{\text{acetone,permeate}} = \frac{J_{\text{acetone,permeate}} \cdot L}{\Delta p_{\text{acetone}}}$$

(4) Tetracycline permeability test

The permeability coefficient of tetracycline was determined to test if large drug molecules can be retained by the membrane. The schematic of this test is shown in Fig. 3-5. Approximately 43 mg of tetracycline was dissolved into 15 mL of methanol. Teflon AF 1600 film was inserted between the two plates of the stainless steel filter holder. On the side that were to be the permeate side, pure methanol was injected by a syringe to fill the space. On the other hand, the tetracycline/methanol solution was injected by a syringe on the side that were to be the feed side. Both ends were plugged and was positioned vertically so that the feed side was at the top and the permeate side at the bottom. It was placed that way overnight to see if there was any permeation of tetracycline occurring. Twenty-four hours later, the solution on the permeate side was analyzed by UV spectrophotometry since tetracycline is detectable by UV. The absorption of the solution was compared with that of pure methanol at 286 nm and 266 nm.

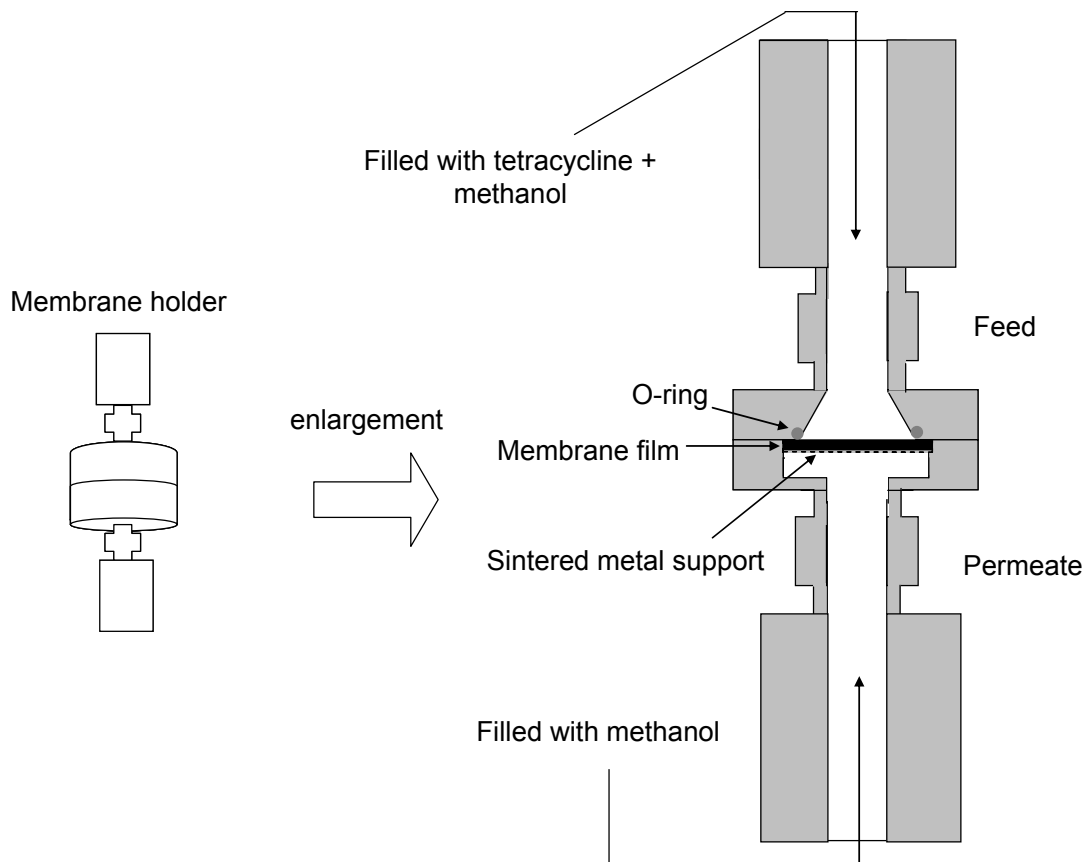


Fig. 3-5. Schematic of tetracycline permeation test

CHAPTER 4

PERMEABILITY OF CARBON DIOXIDE

Calculation of the permeability coefficient of CO₂

The calculation of the permeability coefficient P will be shown below for the data collected at 45 °C and the feed pressure of 231 psig for a Teflon AF 2400 film with a thickness of 63.5 μm . The initial pressure difference Δp was 100 psi, which was the same for all experimental runs. The membrane surface area that was available for permeation was 2.2 cm^2 . The volume on the permeate side was measured to be 14 cm^3 .

First, the calculation of the compressibility factor, z , will be reviewed. Since the permeate pressure (p_p) was varying over time, 3 values of permeate pressure were chosen to calculate z for each permeate pressure. The CO₂ density values of the corresponding permeate pressures were used for the calculation. The 3 calculated compressibility factors were averaged to give one value of z . To get a good average value of z , the first value of the permeate pressure was taken from the beginning of the experiment, the second from the middle of the experiment, and the third from the end of the experiment. The permeate pressure (p_p) chosen as a first value was 138.8 psig, which was taken from the start of the experiment. The calculation of z using this p_p value will be shown as follows. The CO₂ density at 45 °C and 138.8 psig was 0.01841 g/cm^3 . Converting the units of the temperature to K,

$$T = 45^{\circ}\text{C} = (273.15 + 45)\text{K} = 318.15\text{K}$$

Converting the units of the permeate pressure to Pa,

$$p_p = 138.8\text{psig} = (138.8 + 14.7)\text{psia} \times \left(\frac{\text{bar}}{14.51\text{psia}}\right) \times \left(\frac{10^5\text{Pa}}{\text{bar}}\right) = 1.058 \times 10^6\text{Pa}$$

Also converting the units of the CO₂ density into g/m³,

$$\rho_{\text{CO}_2}^{45^{\circ}\text{C}, 138.8\text{psig}} = \left(0.01841 \frac{\text{g}}{\text{cm}^3}\right) \times \left(\frac{10^6\text{cm}^3}{\text{m}^3}\right) = 1.841 \times 10^4 \frac{\text{g}}{\text{m}^3}$$

Using the definition of z, z was calculated:

$$z = \frac{p_p \cdot \text{MW}_{\text{CO}_2}}{RT \cdot \rho_{\text{CO}_2}^{45^{\circ}\text{C}, 138.8\text{psig}}}$$

$$z = \frac{(1.058 \times 10^6\text{Pa}) \cdot \left(44 \frac{\text{g}}{\text{mol}}\right)}{\left(8.314 \frac{\text{Pa} \cdot \text{m}^3}{\text{mol} \cdot \text{K}}\right) (318.15\text{K}) \cdot \left(1.841 \times 10^4 \frac{\text{g}}{\text{m}^3}\right)} = 0.956$$

The first value of z was calculated as 0.956. The other two values were calculated in the same way. The three values was averaged to give one value of z. Averaging, z was obtained to be 0.943.

Next, the value of the slope of the logarithm of the pressure difference vs time, m, will be determined. The graphs are shown in Fig. 4-1a and 4-1b. As the slope of the line, the value of -0.0265min^{-1} was obtained. Converting this units from min^{-1} to sec^{-1} ,

$$m = \left(\frac{-0.0265}{\text{min}}\right) \times \left(\frac{\text{min}}{60\text{sec}}\right) = \frac{-4.42 \times 10^{-4}}{\text{sec}}$$

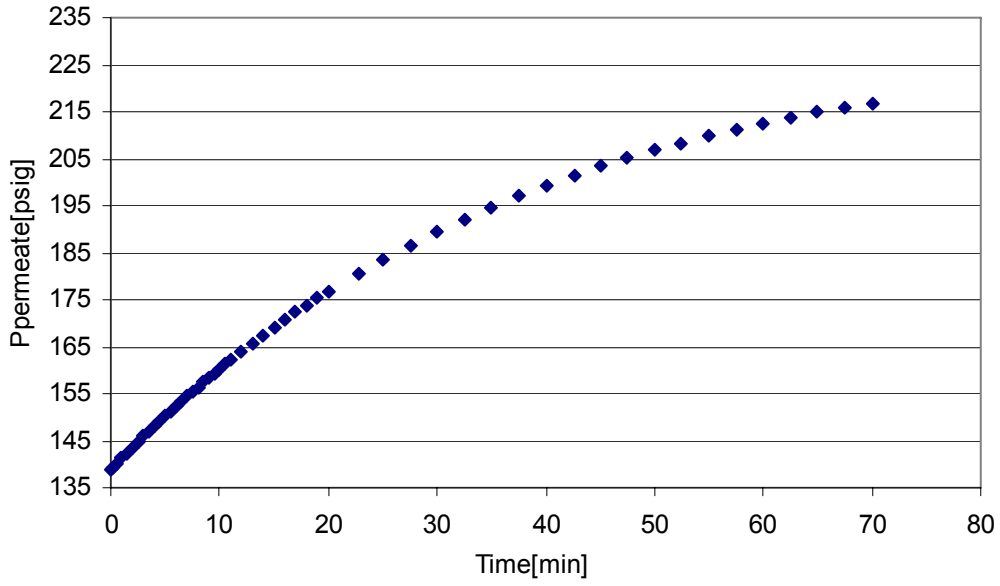


Fig. 4-1a. A graph of permeate pressure vs time for CO₂ permeation through Teflon AF 2400 film with thickness of 63.5 μm. Temperature = 45 °C. Feed pressure = 231 psig. Initial pressure difference = 100 psi.

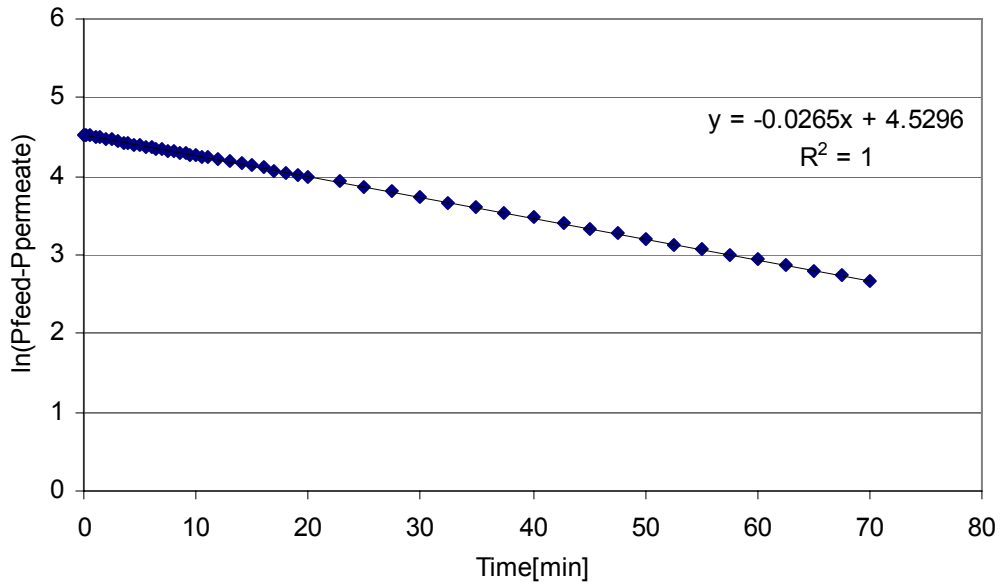


Fig. 4-1b. A graph of logarithm of the pressure difference vs time for CO₂ permeation through Teflon AF 2400 film with thickness of 63.5 μm. Temperature = 45 °C. Feed pressure = 231 psig. Initial pressure difference = 100 psi.

Finally, the permeability coefficient, P , can be calculated. The CO_2 density at STP condition is 0.001977g/cm^3 . The gas constant, R , should be converted to $\text{cmHg} \cdot \text{cm}^3/(\text{mol} \cdot \text{K})$.

$$R = \left(0.08206 \frac{\text{atm} \cdot \text{L}}{\text{mol} \cdot \text{K}}\right) \times \left(\frac{76\text{cmHg}}{\text{atm}}\right) \times \left(\frac{10^3 \text{cm}^3}{\text{L}}\right) = 6237 \frac{\text{cmHg} \cdot \text{cm}^3}{\text{mol} \cdot \text{K}}$$

Converting the units of the film thickness, L , from micrometers (μm) to centimeters (cm),

$$L = (63.5\mu\text{m}) \times \left(\frac{\text{cm}}{10^4 \mu\text{m}}\right) = 6.35 \times 10^{-3} \text{cm}$$

The permeability coefficient, P , can be calculated:

$$P = - \frac{V_p L \cdot \text{MW}_{\text{CO}_2} \cdot m}{zART \cdot \rho_{\text{CO}_2}(\text{STP})} \left[\frac{\text{cm}^3(\text{STP}) \cdot \text{cm}}{\text{s} \cdot \text{cm}^2 \cdot \text{cmHg}} \right]$$

$$P = - \frac{(14\text{cm}^3) \cdot (6.35 \times 10^{-3} \text{cm}) \left(44 \frac{\text{g}}{\text{mol}}\right) \cdot \left(\frac{-4.42 \times 10^{-4}}{\text{sec}}\right)}{(0.943)(2.2\text{cm}^2) \left(6237 \frac{\text{cmHg} \cdot \text{cm}^3}{\text{mol} \cdot \text{K}}\right) (318.15\text{K}) \cdot \left(0.001977 \frac{\text{g}}{\text{cm}^3}\right)}$$

$$= 2.12 \times 10^{-7} \left[\frac{\text{cm}^3(\text{STP}) \cdot \text{cm}}{\text{s} \cdot \text{cm}^2 \cdot \text{cmHg}} \right]$$

$$= 2120[\text{barrer}]$$

The permeability of CO_2 through Teflon AF 2400 film with thickness of $63.5 \mu\text{m}$ was calculated as $2.12 \times 10^{-7} \text{cm}^3(\text{STP}) \cdot \text{cm}/(\text{s} \cdot \text{cm}^2 \cdot \text{cmHg})$ or 2120 barrer while the feed pressure of CO_2 was maintained at 231 psig.

CO₂ permeability in Teflon AF 2400, AF1600 and PTFE

The permeability coefficients of CO₂ in Teflon AF 2400, 1600, and PTFE at 45 °C are tabulated in Table 4-1 and plotted against feed pressure in Fig. 4-2.

Table 4-1. CO₂ permeability coefficients in different membranes vs feed pressure at 45 °C and initial pressure difference of 100 psi

Teflon AF 2400						
Pfeed [psig]	231	430	629	829	1173	1270
Permeability [barrer]	2120	2450	3100	3680	3350	2700

Teflon AF 1600						
Pfeed [psig]	230	428	627			
Permeability [barrer]	630	1210	1820			

PTFE						
Pfeed [psig]	232				1273	
Permeability [barrer]	16				16	

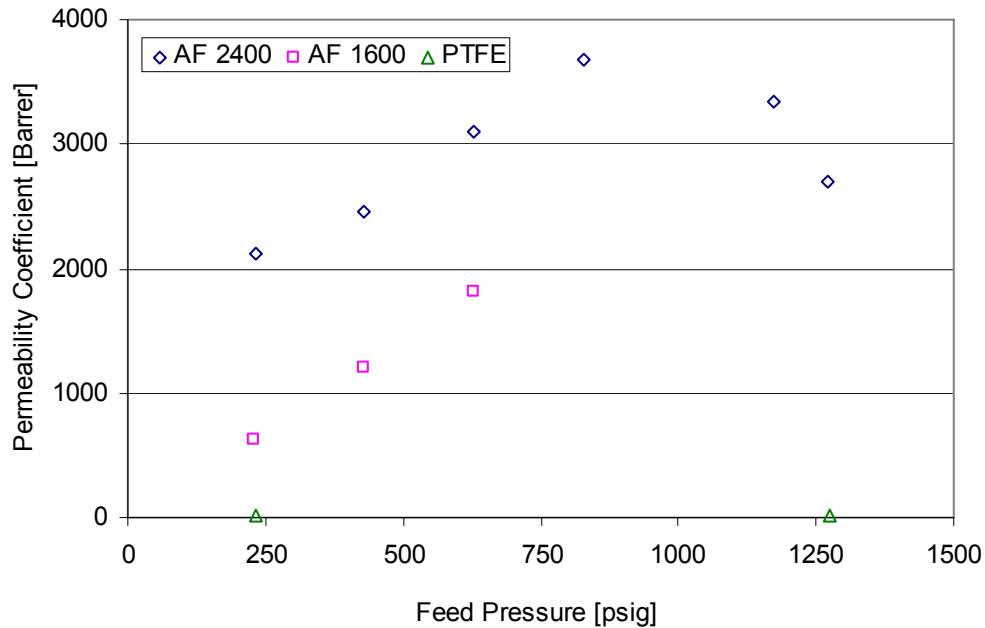


Fig. 4-2. CO₂ permeability coefficients in different membranes vs feed pressure at 45 °C and initial pressure difference of 100 psi

Teflon AF 2400 had a permeability value ranging in 2100-3700 barrer for the feed pressures of 230-1270 psig. Up to the feed pressure of 830 psig, the permeability coefficient increased as the feed pressure increased, but for 1170 psig, the value dropped and dropped further for 1270 psig. It can be said that a maximum value for the permeability coefficient exists between 830 psig and 1170 psig. Between these pressures, critical pressure of CO₂ exists.

This type of maximum permeability of CO₂ was observed by Patil et al [2006] as well. They observed a maximum permeability of CO₂ through 1-2 μm thick polyvinyl alcohol (PVA) membrane and 0.5-1 μm thick polyamide copolymer (IPC) membrane at the pressure very close to the critical pressure of CO₂ when the experiment was performed at the temperature of 40 °C and pressure difference of 0.3 MPa. Their

conclusion was that the transport mechanism through the membrane followed the Hagen-Poiseuille model [Bird et al., 2002; Mulder, 1996], which is generally applied for viscous flow where the interaction between the molecules is more dominant than the interaction between the molecules and the pore wall. Hagen-Poiseuille equation is:

$$J = \left(\frac{\varepsilon}{\tau}\right) \left(\frac{r^2}{8L \cdot MW}\right) \left(\frac{\rho}{\mu}\right) \Delta p$$

where J is the flux of the penetrant, ε the porosity, τ the pore tortuosity, ρ the density of the penetrant, μ the absolute viscosity of the penetrant, r the pore radius, L the membrane thickness, MW the molecular weight of the penetrant and Δp the pressure difference across the membrane. Since Hagen-Poiseuille equation generally describes the scheme of the flow through pipes, it can be said that the assumption was made for the pores to have a cylindrical structure and equal radius. In seen in the equation, the ratio of the density to viscosity (inverse of the kinematic viscosity) is a critical parameter. The density of CO₂ drastically changes about the critical pressure and so does the viscosity. The rates at which density and viscosity change with feed pressure affect the value of the ratio and hence, the permeability. This may have lead to the existence of maximum in the permeability value. From the permeability data of CO₂ and N₂ through IPC membrane, they have back-calculated the membrane pore size and obtained the value of 1.9 nm and 1.7 nm respectively.

It is assumed that the pore size of Teflon AFs is in the range of 5.9-6.4 Å [Alentiev et al., 1997] and is smaller than 1.7 nm (17 Å) so Hagen-Poiseuille model may not be appropriate to apply. Further discussion will be required to explain the existence of maximum permeability.

Teflon AF 1600 had a permeability value ranging in 630-1820 barrer for the feed pressures of 230-630 psig. The permeability coefficient increased as the feed pressure increased.

Polytetrafluoroethylene (PTFE) had a permeability value of 16 barrer at the feed pressure of 230 psig and 1270 psig. There was scarcely any permeation compared to the Teflon AF products.

Comparing the permeability among the three polymers, it can be easily seen that Teflon AF 2400 has the highest permeability among the three, followed by AF 1600 and then PTFE. The fact that Teflon AF 2400 has a higher permeability than AF 1600 can be explained by the difference in the amount of free volume in the polymers. AF 2400 has higher free volume than AF 1600. The large difference in the permeability of Teflon AF products and PTFE can be explained by the degree of crystallinity. As gas/vapor transport occurs through the amorphous part of the polymer, the portion at which this can happen is limited for PTFE. This permeability result can be comprehended in terms of the amount of tetrafluoroethylene (TFE) in the polymer that the permeability decreases as the ratio of tetrafluoroethylene increases. In terms of the amount of 2,2-bis(trifluoromethyl)-4,5-difluoro-1,3-dioxole (PDD) in the polymer, the permeability increases as the ratio of PDD increases. Hence, it can be said that the PDD structure contributes to the decrease in crystallinity and increase in free volume, leading to an increase in CO₂ permeability.

In Table 4-2, the permeability coefficient of Teflon AF 2400 obtained by previous studies was organized along with the value obtained in this work. The value obtained in the current work fell in the same range as the values obtained by other researchers. The differences in the values obtained can be attributed to the difference in the formation of the membrane and the difference in the experimental condition or method.

Table 4-2. CO₂ Permeability coefficients in Teflon AF 2400 studied previously

Reference	P [barrer]	T [°C]	p_f [MPa]	Δp [MPa]
Current work	2440	50	2.9	0.69
Current work	2450	45	3.1	0.69
Current work	2590	40	3.2	0.69
Current work	2740	35	3.3	0.69
S. M. Nemser, 1991	2800	25	1.7	1.6
I. Pinnau, 1996	3900	25	0.45	0.35
A. Y. Alentiev, 1997	2600	22	0.013-0.037	0.013-0.037
T. C. Merkel, 1999	2200	35		0

Current work, 2006: polymer purchased from Random Technologies

S. M. Nemser, 1991: melt-pressed

I. Pinnau, 1996: solvent cast from perfluoro-N-methyl morpholine (PF 5052), air-dried overnight at ambient condition, dried in a vacuum oven at 150 °C for 3 days

A. Y. Alentiev, 1997: cast from perfluorotoluene, dried at 55 °C, dried in a vacuum oven at 40-50 °C

T. C. Merkel, 1999: cast from PF 5060, dried at ambient condition

Temperature dependence of CO₂ permeability through Teflon AF 2400

Fig. 4-3a depicts the permeability coefficients in Teflon AF 2400 versus feed pressure (220-830 psig) at various temperatures (35-50 °C) to see if there is any temperature dependence of the permeability. Fig. 4-3b is the Arrhenius plot of CO₂ permeability in Teflon AF 2400. From the graphs obtained, it can be said that there is not a significant dependence on temperature, although there seems to be a slight decrease in permeability as the temperature increases. This matches with Pinnau et al. (1996)'s work where they have found that only a weak temperature dependence of permeability is shown for Teflon AF 2400.

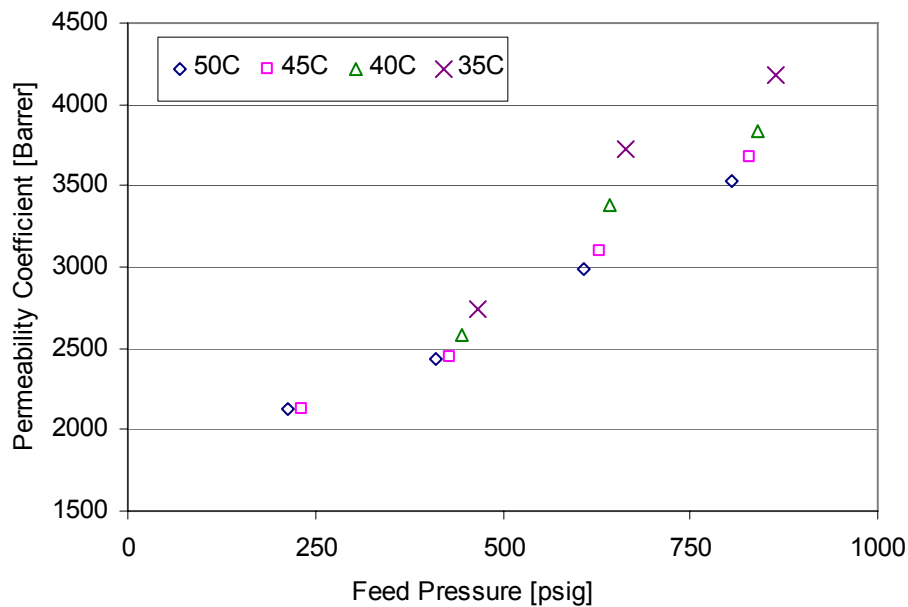


Fig. 4-3a. Temperature dependence of CO₂ permeability in Teflon AF 2400 film at varying feed pressure. Initial pressure difference = 100 psi.

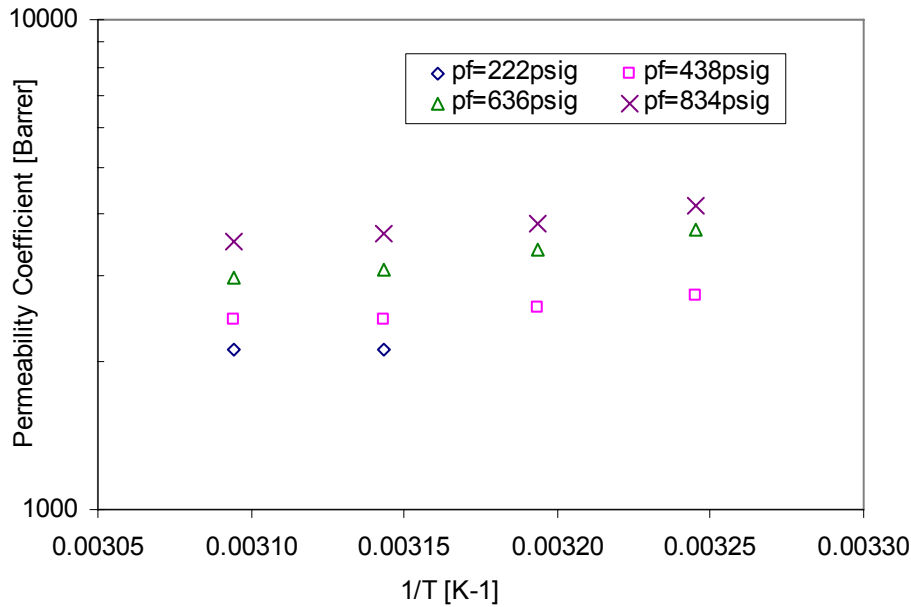


Fig. 4-3b. Arrhenius plot of CO₂ permeability in Teflon AF 2400 film at varying feed pressure. Initial pressure difference = 100 psi.

CO₂ plasticization effect on Teflon AF 2400 and AF 1600

Bos et al. [1999] defined plasticization as an increase in permeability as a function of feed pressure. The pressure at which plasticization occurs is called the plasticization pressure. Fig. 4-4a shows the plasticization effect of CO₂ on Teflon AF 2400 and Fig. 4-4b shows for AF 1600 at 45 °C. First-time-use membrane showed a profile that increased as the feed pressure increased, but as the membrane is used for the second run, third run, and so on, the permeability coefficients became independent of the feed pressure. Although to a smaller degree, the same trend can be seen for AF 1600, where the permeability coefficients became less dependent on the feed pressure as the membrane is used more. This plasticization phenomenon can be attributed to CO₂ acting as a swelling agent and increasing segmental mobility of the polymer, resulting in an increase of free

volume. The difference in the degree of plasticization between AF 2400 and AF 1600 may be due to the difference in the amount of free volume in the polymers. Since 2,2-bistrifluoromethyl-4,5-difluoro-1,3-dioxole (PDD) in the polymer contributes greatly to the amount of free volume, with AF 2400 having 87% PDD and AF 1600 having 65% PDD, the free volume is higher for AF 2400. The higher free volume led to a higher degree of plasticization, even reaching the point where the permeability became independent of the feed pressure.

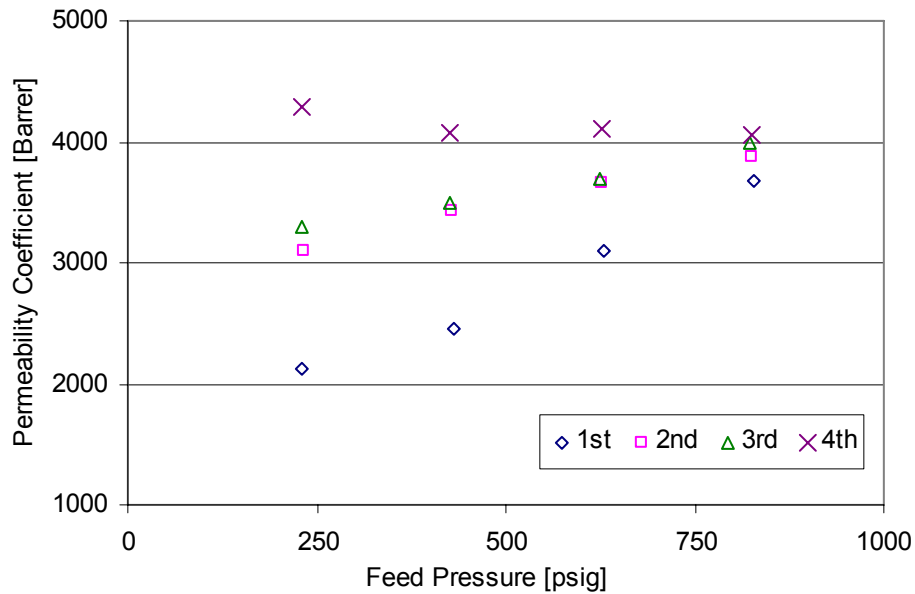


Fig. 4-4a. Plasticization effect on CO₂ permeability in Teflon AF 2400 film at 45 °C. Initial pressure difference = 100 psi.

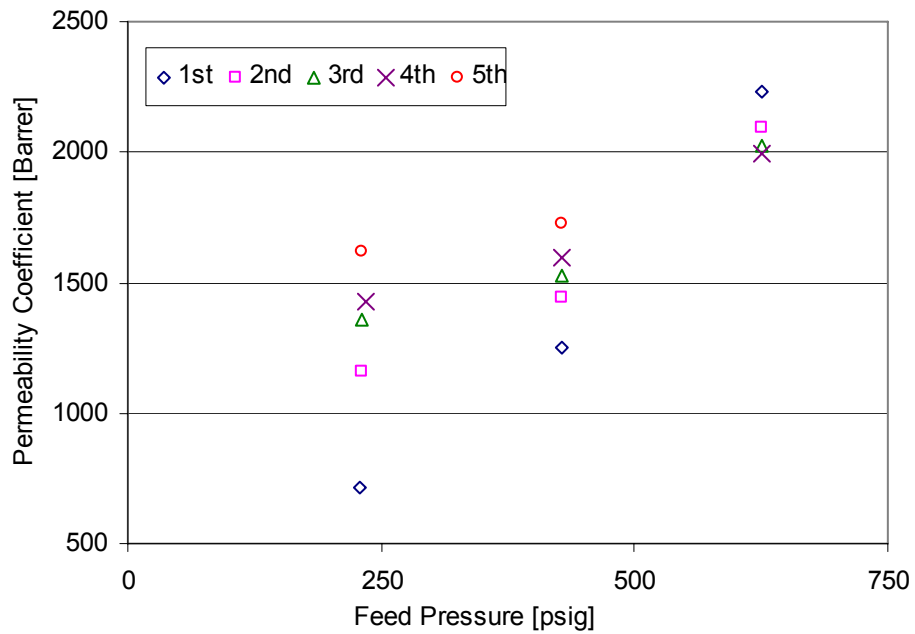


Fig. 4-4b. Plasticization effect on CO₂ permeability in Teflon AF 1600 film at 45 °C. Initial pressure difference = 100 psi.

CHAPTER 5

PERMEABILITY OF ACETONE

Verification of the measurement

The verification of the measurement was performed on the set-up for the acetone + CO₂ permeation test at 40 °C. The sample solution (acetone + CO₂) collected at the 6-port valve was analyzed by UV spectrophotometry to determine the weight of acetone collected. This value was then compared with the theoretical value that should have been collected in the loop of the 6-port valve, applying the assumption that 100 % of acetone fed was maintained within the system. Fig. 5-1 shows the calibration curve for acetone solutions of known concentrations. The net absorption was taken on the x-axis and the acetone concentration in the units of grams acetone per grams solution (g acetone/g solution) was taken on the y-axis. The net absorption refers to the difference in absorptivity measured at 500 nm and 266 nm. (Acetone shows absorption at 266 nm.) The equation for the calibration line turned out to be $y = 0.0033x - 3 \times 10^{-5}$ with the linearity being very high.

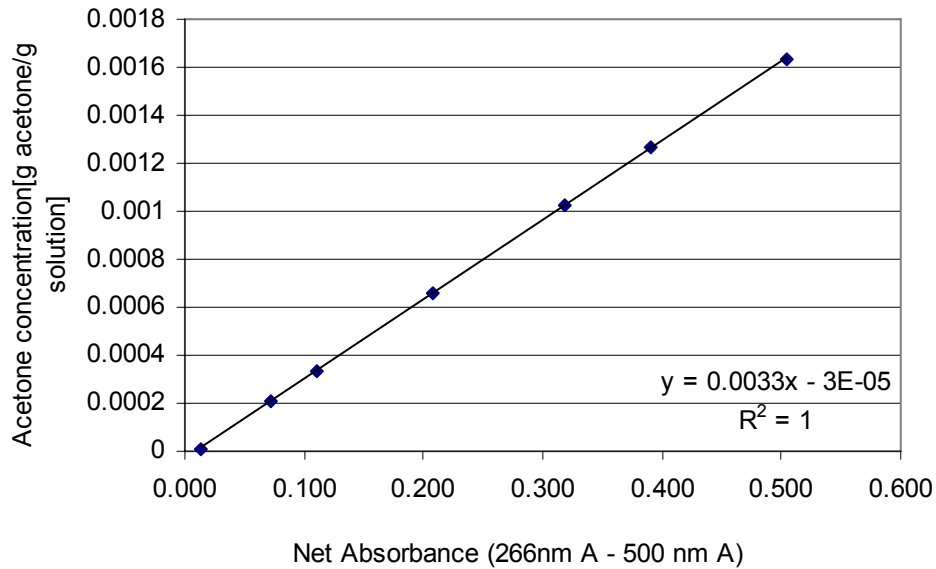


Fig. 5-1. UV calibration curve for acetone

Using this calibration line, the concentration of the solution (y) collected at the 6-port valve was determined from the net absorption (x) obtained by the ultraviolet (UV) spectrophotometric analysis. The calculation for the percentage of acetone collected at the 6-port valve will be shown below. First, the amount of acetone fed into the system will be calculated to determine the mole fraction of acetone in the acetone + CO₂ feed flow y_{acetone} . The mass flow rate of acetone fed, $m_{\text{acetone, fed}}$, was calculated from the volumetric flow rate of acetone at 27 °C, $v_{\text{acetone, fed}}^{27^\circ\text{C}}$:

$$m_{\text{acetone, fed}} = \rho_{\text{acetone}}^{27^\circ\text{C}} \cdot v_{\text{acetone, fed}}^{27^\circ\text{C}}$$

$$m_{\text{acetone, fed}} = \left(0.783 \frac{\text{g}}{\text{mL}} \right) \cdot \left(0.25 \frac{\text{mL}}{\text{min}} \right) = 0.1958 \frac{\text{g}}{\text{min}}$$

The mass flow rate of acetone that was fed, $m_{\text{acetone, fed}}$, was calculated as 0.1958 g/min.

Next, the molar flow rate of acetone fed, $n_{\text{acetone, fed}}$, was calculated:

$$n_{\text{acetone, fed}} = \frac{m_{\text{acetone, fed}}}{\text{MW}_{\text{acetone}}}$$

$$n_{\text{acetone, fed}} = \frac{0.1958 \frac{\text{g}}{\text{min}}}{58 \frac{\text{g}}{\text{mol}}} = 0.003376 \frac{\text{mol}}{\text{min}}$$

The molar flow rate of acetone that was fed into the system, $m_{\text{acetone, fed}}$, was calculated as 0.003376 mol/min. The mass and molar flow rate of CO₂ fed into the system was calculated in the same way. The system pressure p was 8.51 MPa and the CO₂ volumetric flow rate at 40 °C and 8.51 MPa, $v_{\text{CO}_2, \text{ fed}}^{40^\circ\text{C}, 8.51\text{MPa}}$, was 4.3 mL/min. The CO₂ density at that condition, $\rho_{\text{CO}_2}^{40^\circ\text{C}, 8.51\text{MPa}}$, was 0.356 g/mL.

$$m_{\text{CO}_2, \text{ fed}} = \rho_{\text{CO}_2}^{40^\circ\text{C}, 8.51\text{MPa}} \cdot v_{\text{CO}_2, \text{ fed}}^{40^\circ\text{C}, 8.51\text{MPa}}$$

$$m_{\text{CO}_2, \text{ fed}} = \left(0.356 \frac{\text{g}}{\text{mL}}\right) \cdot \left(4.3 \frac{\text{mL}}{\text{min}}\right) = 1.53 \frac{\text{g}}{\text{min}}$$

The mass flow rate of CO₂ fed into the system, $m_{\text{CO}_2, \text{ fed}}$, was calculated as 1.53 g/min.

$$n_{\text{CO}_2, \text{ fed}} = \frac{m_{\text{CO}_2, \text{ fed}}}{\text{MW}_{\text{CO}_2}}$$

$$n_{\text{CO}_2, \text{ fed}} = \frac{1.53 \frac{\text{g}}{\text{min}}}{44 \frac{\text{g}}{\text{mol}}} = 0.0348 \frac{\text{mol}}{\text{min}}$$

The molar flow rate of CO₂ fed into the system, $n_{\text{CO}_2, \text{fed}}$, was calculated as 0.0348 mol/min. Now, the mole fraction of acetone in acetone + CO₂ feed flow, $y_{\text{acetone, fed}}$, can be calculated:

$$y_{\text{acetone, fed}} = \frac{n_{\text{acetone, fed}}}{n_{\text{acetone, fed}} + n_{\text{CO}_2, \text{fed}}}$$

$$y_{\text{acetone, fed}} = \frac{0.00338 \frac{\text{mol}}{\text{min}}}{0.00338 \frac{\text{mol}}{\text{min}} + 0.0348 \frac{\text{mol}}{\text{min}}} = 0.0884$$

The mole fraction of acetone in acetone + CO₂ feed flow, $y_{\text{acetone, fed}}$, was calculated as 0.0884. From pressure p (8.51 MPa), temperature T (40 °C) and acetone mole fraction in the acetone + CO₂ feed flow, $y_{\text{acetone, fed}}$, the compressibility factor z can be calculated using Peng-Robinson Equation of State (PR-EOS). Using the PR-EOS program, z was calculated as 0.2019.

The molar volume of the feed mixture (acetone + CO₂), $v_{\text{mol, mixt}}$, can be calculated from the compressibility equation. The conversions were done in advance. Converting the system pressure $p = 8.51 \text{ MPa}$ into the units of atm,

$$p = (8.51 \text{ MPa}) \times \left(\frac{10^6 \text{ Pa}}{\text{MPa}} \right) \times \left(\frac{\text{atm}}{1.013 \times 10^5 \text{ Pa}} \right) = 84.0 \text{ atm}$$

The molar volume of the feed mixture, $v_{\text{mol, mixt}}$, will be calculated:

$$v_{\text{mol, mixt}} = \frac{zRT}{p}$$

$$v_{\text{mol,mixt}} = \frac{(0.202) \left(0.08206 \frac{\text{atm} \cdot \text{L}}{\text{mol} \cdot \text{K}} \right) (313.15\text{K})}{84.0\text{atm}} = 0.0618 \frac{\text{L}}{\text{mol}}$$

Changing the units from L/mol to cm³/mol,

$$v_{\text{mol,mixt}} = \left(0.0618 \frac{\text{L}}{\text{mol}} \right) \left(\frac{10^3 \text{cm}^3}{\text{L}} \right) = 61.8 \frac{\text{cm}^3}{\text{mol}}$$

The molar volume of the feed mixture, $v_{\text{mol,mixt}}$, was calculated as 61.77 cm³/mol. Inverse

of $v_{\text{mol,mixt}}$ is the molar density, $\rho_{\text{mol,mixt}}$:

$$\rho_{\text{mol,mixt}} = \frac{1}{v_{\text{mol,mixt}}}$$

$$\rho_{\text{mol,mixt}} = \frac{1}{\left(61.8 \frac{\text{cm}^3}{\text{mol}} \right)} = 0.0162 \frac{\text{mol}}{\text{cm}^3}$$

To calculate the weight density of the mixture, the molecular weight of the feed mixture needs to be calculated. The molecular weight of the mixture, MW_{mixt} , can be calculated as:

$$\text{MW}_{\text{mixt}} = (\text{MW}_{\text{acetone}})(y_{\text{acetone, fed}}) + (\text{MW}_{\text{CO}_2})(y_{\text{CO}_2, \text{ fed}})$$

$$\text{MW}_{\text{mixt}} = (\text{MW}_{\text{acetone}})(y_{\text{acetone, fed}}) + (\text{MW}_{\text{CO}_2})(1 - y_{\text{acetone, fed}})$$

$$\text{MW}_{\text{mixt}} = \left(58 \frac{\text{g}}{\text{mol}} \right) (0.0884) + \left(44 \frac{\text{g}}{\text{mol}} \right) (1 - 0.0884) = 45.2 \frac{\text{g}}{\text{mol}}$$

Now, the weight density of the feed mixture, $\rho_{\text{g,mixt}}$, can be calculated:

$$\rho_{\text{g,mixt}} = (\rho_{\text{mol,mixt}})(\text{MW}_{\text{mixt}})$$

$$\rho_{\text{g,mixt}} = \left(0.0162 \frac{\text{mol}}{\text{cm}^3} \right) \left(45.2 \frac{\text{g}}{\text{mol}} \right) = 0.732 \frac{\text{g}}{\text{cm}^3}$$

If the assumption is made that the acetone fed was 100 % maintained within the system, from the weight density of the mixture, $\rho_{g,mixt}$, and the acetone mole fraction, $y_{acetone, fed}$, in the combined flow, the amount of acetone that should have been collected in the sample loop volume of 0.19 cm^3 , $w_{acetone_fed_loop}$, can be calculated as:

$$w_{acetone_fed_loop} = \frac{(\rho_{g,mixt})(v_{loop})(y_{acetone, fed})(MW_{acetone})}{MW_{mixt}}$$

$$w_{acetone_fed_loop} = \frac{\left(0.732 \frac{\text{g}}{\text{cm}^3}\right)(0.19\text{cm}^3)(0.0884)(58 \frac{\text{g}}{\text{mol}})}{\left(45.2 \frac{\text{g}}{\text{mol}}\right)} = 0.0158\text{g}$$

This is the value of the weight of acetone that should have been collected at the loop of the 6-port valve, calculated from the amount of acetone fed into the system and assuming that 100 % of the acetone fed into the system was maintained within the system, and it was calculated as 0.0158 g. This acetone amount was compared with the amount that was collected at the 6-port valve and analyzed by UV experimentally. The weight of acetone in the loop obtained from UV analysis was 0.0162 g. Therefore, the percentage of the acetone collected at the 6-port valve is:

$$\text{Percentage} = \frac{w_{acetone_UV_loop}}{w_{acetone_fed_loop}} \times 100\%$$

$$\text{Percentage} = \frac{0.0162\text{g}}{0.0158\text{g}} \times 100\% = 103\%$$

In Table 5-1, the result is summarized for the set-up verification experiments. The percentage of the acetone collected ranged from 103-110 %. It can be said that there was no leak in the system and the data obtained in this method is trustable.

Table 5-1. Verification of set-up for acetone + CO₂ permeation

Run number	Pressure [MPa]	CO ₂ feed flow rate at 40°C, p [mL/min]	Acetone feed flow rate at 27°C [mL/min]	Acetone collected [g]	Acetone fed [g]	Percentage collected [%]
1	8.508	4.3	0.25	0.0162	0.0158	103
2	8.644	3.8	0.25	0.0173	0.0164	105
3	9.607	2.3	0.10	0.00791	0.0072	110
4	8.247	4.1	0.10	0.00760	0.0071	107

Measurement of acetone permeation

Calculation of the percentage of feed acetone that permeated through the membrane

Acetone permeation test was performed on Teflon AF 1600 film with thickness of 40.6 μm at 40 °C. The calculation of the percentage of acetone that permeated through Teflon AF 1600 film will be shown below. To calculate what percentage of the feed acetone permeated through the membrane, the amount of acetone collected at the 6-port valve on the permeate side will be compared with the amount of acetone fed into the system. The amount of acetone fed into the system will be calculated as follows. The calculation will be shown here for the experiment in which the volumetric flow rate of the feed acetone was 0.50 mL/min at 25 °C and the volumetric flow rate of the feed CO₂ was 227 mL/min at 40 °C and 1 atm. The CO₂ pressure on both the permeate and the retentate side was maintained at 3.21 MPa. The density of the acetone at 25 °C was 0.783 g/mL and the density of CO₂ at 40 °C and 1 atm was 0.00172 g/mL

(<http://webbook.nist.gov>). First, the mole fraction of acetone in the CO₂ + acetone feed flow, $y_{\text{acetone, fed}}$, will be calculated as:

$$y_{\text{acetone, fed}} = \frac{\frac{(\rho_{\text{acetone}}^{25^\circ\text{C}})(v_{\text{acetone, fed}}^{25^\circ\text{C}})}{\text{MW}_{\text{acetone}}}}{\frac{(\rho_{\text{acetone}}^{25^\circ\text{C}})(v_{\text{acetone, fed}}^{25^\circ\text{C}})}{\text{MW}_{\text{acetone}}} + \frac{(\rho_{\text{CO}_2}^{40^\circ\text{C}, 1\text{atm}})(v_{\text{CO}_2, \text{ fed}}^{40^\circ\text{C}, 1\text{atm}})}{\text{MW}_{\text{CO}_2}}}$$

$$y_{\text{acetone, fed}} = \frac{\left(0.783 \frac{\text{g}}{\text{mL}}\right)\left(0.50 \frac{\text{mL}}{\text{min}}\right)}{\left(58 \frac{\text{g}}{\text{mol}}\right)} = 0.4321$$

$$y_{\text{acetone, fed}} = \frac{\left(0.783 \frac{\text{g}}{\text{mL}}\right)\left(0.50 \frac{\text{mL}}{\text{min}}\right)}{\left(58 \frac{\text{g}}{\text{mol}}\right)} + \frac{\left(0.00172 \frac{\text{g}}{\text{mL}}\right)\left(227 \frac{\text{mL}}{\text{min}}\right)}{\left(44 \frac{\text{g}}{\text{mol}}\right)}$$

From pressure, p , temperature, T , and acetone mole fraction in the feed flow, $y_{\text{acetone, fed}}$, the compressibility factor, z , can be calculated using Peng-Robinson Equation of State (PR-EOS).

After obtaining z using the PR-EOS program, the molar volume of the feed mixture, $v_{\text{mol, mixt}}$, can be calculated from the compressibility equation. First, converting the system pressure $p = 3.21 \text{ MPa}$ into the units of atm,

$$p = (3.21 \text{ MPa}) \times \frac{10^6 \text{ Pa}}{\text{MPa}} \times \frac{\text{atm}}{1.013 \times 10^5 \text{ Pa}} = 31.7 \text{ atm}$$

The molar volume of the feed mixture, $v_{\text{mol, mixt}}$, can be calculated:

$$v_{\text{mol, mixt}} = \frac{zRT}{p}$$

$$v_{\text{mol,mixt}} = \frac{(0.07984) \left(0.08206 \frac{\text{atm} \cdot \text{L}}{\text{mol} \cdot \text{K}} \right) (313.15\text{K})}{31.7\text{atm}} = 0.0647 \frac{\text{L}}{\text{mol}}$$

Changing the units from L/mol to cm³/mol,

$$v_{\text{mol,mixt}} = \left(0.0647 \frac{\text{L}}{\text{mol}} \right) \left(\frac{10^3 \text{ cm}^3}{\text{L}} \right) = 64.7 \frac{\text{cm}^3}{\text{mol}}$$

Inverse of $v_{\text{mol,mixt}}$ is the molar density, $\rho_{\text{mol,mixt}}$:

$$\rho_{\text{mol,mixt}} = \frac{1}{v_{\text{mol,mixt}}}$$

$$\rho_{\text{mol,mixt}} = \frac{1}{64.7 \frac{\text{cm}^3}{\text{mol}}} = 0.0155 \frac{\text{mol}}{\text{cm}^3}$$

The weight density, $\rho_{\text{g,mixt}}$, can be obtained by multiplying the molecular weight of the mixture MW_{mixt} with the molar density $\rho_{\text{mol,mixt}}$. First, the molecular weight of the mixture will be calculated:

$$MW_{\text{mixt}} = (MW_{\text{acetone}})(y_{\text{acetone, fed}}) + (MW_{\text{CO}_2})(y_{\text{CO}_2, \text{fed}})$$

$$= (MW_{\text{acetone}})(y_{\text{acetone, fed}}) + (MW_{\text{CO}_2})(1 - y_{\text{acetone, fed}})$$

$$MW_{\text{mixt}} = (58 \frac{\text{g}}{\text{mol}})(0.432) + (44 \frac{\text{g}}{\text{mol}})(1 - 0.432) = 50.1 \frac{\text{g}}{\text{mol}}$$

Hence, the weight density of the mixture, $\rho_{\text{g,mixt}}$, can be calculated:

$$\rho_{\text{g,mixt}} = (\rho_{\text{mol,mixt}})(MW_{\text{mixt}})$$

$$\rho_{\text{g,mixt}} = (0.0155 \frac{\text{mol}}{\text{cm}^3})(50.1 \frac{\text{g}}{\text{mol}}) = 0.773 \frac{\text{g}}{\text{cm}^3}$$

If the assumption is made that 100 % of the feed acetone permeated through the membrane, from the weight density of the mixture, $\rho_{g,mixt}$, and the acetone mole fraction in the combined feed flow, $y_{acetone, fed}$, the weight of acetone that is to be collected in the loop, $w_{acetone_fed_loop}$, can be calculated as:

$$w_{acetone_fed_loop} = \frac{(\rho_{g,mixt})(v_{loop})(y_{acetone, fed})(MW_{acetone})}{MW_{mixt}}$$

$$w_{acetone_fed_loop} = \frac{(0.773 \frac{g}{cm^3})(0.19cm^3)(0.432)(58 \frac{g}{mol})}{50.1 \frac{g}{mol}} = 0.0736g$$

This acetone amount should be compared with the amount obtained from UV analysis.

Percentage of acetone that permeated through the membrane is calculated:

$$\text{Percentage} = \frac{w_{acetone_UV_loop}}{w_{acetone_fed_loop}} \times 100$$

$$\text{Percentage} = \frac{0.00517g}{0.0736g} \times 100\% = 7\%$$

Table 5-2. shows the percentage of feed acetone that permeated through Teflon AF 1600 film of 40.6 μm thickness.

Table 5-2. Acetone amount collected in 0.19 mL volume and percentage of feed acetone that permeated through Teflon AF 1600 film of 40.6 μm thickness at 40 °C

Pressure [MPa]	CO ₂ feed flow rate at 40°C, 1atm [mL/min]	Acetone feed flow rate at 25°C [mL/min]	Acetone permeated [g]	Acetone fed [g]	Percentage permeated [%]
3.21	227	0.50	0.00517	0.0735	7

Calculation of acetone permeation flux and permeability coefficient

The following will be the calculation of the permeation flux and the permeability coefficient of acetone through Teflon AF 1600 film. The CO₂ flow rate at the permeate and the retentate side were measured with inversed cylinder at the exit of the restrictors in the 40 °C water bath. Hence, the CO₂ volumetric flow rates on the permeate and the retentate side were measured at 40 °C and ambient pressure (1 atm). The volumetric flow rate at 40 °C and 1 atm was 180 mL/min for the permeate side and 47 mL/min for the retentate side of the membrane.

$$v_{\text{CO}_2, \text{permeate}}^{40^\circ\text{C}, 1\text{atm}} = 180 \frac{\text{mL}}{\text{min}}$$

$$v_{\text{CO}_2, \text{retentate}}^{40^\circ\text{C}, 1\text{atm}} = 47 \frac{\text{mL}}{\text{min}}$$

These volumetric flow rates can be converted into mass flow rates by multiplying the CO₂ density at that condition (40 °C and 1 atm). The values of the density of CO₂ at the certain pressure and 40 °C were obtained from NIST webbook. From the density of CO₂ at 40 °C and 1 atm, $\rho_{\text{CO}_2}^{40^\circ\text{C}, 1\text{atm}}$, which is 0.00172 g/mL,

$$m_{\text{CO}_2, \text{permeate}} = v_{\text{CO}_2, \text{permeate}}^{40^\circ\text{C}, 1\text{atm}} \times \rho_{\text{CO}_2}^{40^\circ\text{C}, 1\text{atm}}$$

$$m_{\text{CO}_2, \text{permeate}} = \left(180 \frac{\text{mL}}{\text{min}}\right) \times \left(0.00172 \frac{\text{g}}{\text{mL}}\right) = 0.3096 \frac{\text{g}}{\text{min}}$$

$$m_{\text{CO}_2, \text{retentate}} = v_{\text{CO}_2, \text{retentate}}^{40^\circ\text{C}, 1\text{atm}} \times \rho_{\text{CO}_2}^{40^\circ\text{C}, 1\text{atm}}$$

$$m_{\text{CO}_2, \text{retentate}} = \left(47 \frac{\text{mL}}{\text{min}}\right) \times \left(0.00172 \frac{\text{g}}{\text{mL}}\right) = 0.08084 \frac{\text{g}}{\text{min}}$$

The mass flow rate of CO₂ on the permeate side, $m_{\text{CO}_2, \text{permeate}}$, and the retentate side, $m_{\text{CO}_2, \text{retentate}}$, were calculated as 0.3096g/min and 0.08084g/min respectively.

Dividing the CO₂ mass flow rate on the permeate side by the CO₂ density at the system condition (40 °C and 3.21 MPa), CO₂ volumetric flow rate can be obtained at the system condition:

$$v_{\text{CO}_2, \text{permeate}}^{40^\circ\text{C}, 3.21\text{MPa}} = \frac{m_{\text{CO}_2, \text{permeate}}}{\rho_{\text{CO}_2}^{40^\circ\text{C}, 3.21\text{MPa}}}$$

$$v_{\text{CO}_2, \text{permeate}}^{40^\circ\text{C}, 3.21\text{MPa}} = \frac{\left(0.3096 \frac{\text{g}}{\text{min}}\right)}{\left(0.06378 \frac{\text{g}}{\text{mL}}\right)} = 4.85 \frac{\text{mL}}{\text{min}}$$

Hence, the CO₂ volumetric flow rate on the permeate side at the system condition, $v_{\text{CO}_2, \text{permeate}}^{40^\circ\text{C}, 3.21\text{MPa}}$, was calculated as 4.85mL/min.

From the UV analysis, the weight of acetone collected in the sample loop of the 6-port valve at the permeate side was obtained. The amount of acetone collected in the sample loop volume of 0.19 mL at 3.21 MPa and 40 °C, $w_{\text{acetone_UV_loop}}$, was 0.00517 g.

Dividing this amount by the sample loop volume will give the concentration (w/v) of acetone in the CO₂ + acetone solution collected in the loop.

$$c_{\text{acetone, permeate}}^{40^\circ\text{C}, 3.21\text{MPa}} = \frac{w_{\text{acetone_UV_loop}}}{V_{\text{loop}}}$$

$$c_{\text{acetone, permeate}}^{40^\circ\text{C}, 3.21\text{MPa}} = \frac{0.00517\text{g}}{0.19\text{mL}} = 0.02721 \frac{\text{g}}{\text{mL}}$$

Assuming that acetone is sparing amount compared to CO₂, the CO₂ volumetric flow rate can be considered as the volumetric flow rate of the CO₂ + acetone flow at the system condition.

$$v_{\text{CO}_2 + \text{acetone, permeate}}^{40^\circ\text{C}, 3.21\text{MPa}} = v_{\text{CO}_2, \text{permeate}}^{40^\circ\text{C}, 3.21\text{MPa}} = 4.854 \frac{\text{mL}}{\text{min}}$$

Multiplying the acetone concentration, $c_{\text{acetone, permeate}}^{40^\circ\text{C}, 3.21\text{MPa}}$, with the volumetric flow rate $v_{\text{CO}_2 + \text{acetone, permeate}}^{40^\circ\text{C}, 3.21\text{MPa}}$ gives the mass flow rate of acetone that permeated through the membrane $m_{\text{acetone, permeate}}$.

$$m_{\text{acetone, permeate}} = c_{\text{acetone, permeate}}^{40^\circ\text{C}, 3.21\text{MPa}} \times v_{\text{CO}_2 + \text{acetone, permeate}}^{40^\circ\text{C}, 3.21\text{MPa}}$$

$$m_{\text{acetone, permeate}} = \left(0.02721 \frac{\text{g}}{\text{mL}}\right) \times \left(4.854 \frac{\text{mL}}{\text{min}}\right) = 0.132 \frac{\text{g}}{\text{min}}$$

Next, the acetone amount that was fed to the feed side will be considered. The mass flow rate of acetone fed into the system by the liquid pump at ambient temperature, $m_{\text{acetone, feed}}$, can be calculated using the acetone density value at ambient temperature, 25 °C ($\rho_{\text{acetone}}^{25^\circ\text{C}} = 0.7855 \text{ g/mL}$). Since acetone was run at 0.50 mL/min at 25 °C,

$$m_{\text{acetone, feed}} = v_{\text{acetone}}^{25^\circ\text{C}} \times \rho_{\text{acetone}}^{25^\circ\text{C}}$$

$$m_{\text{acetone, feed}} = \left(0.50 \frac{\text{mL}}{\text{min}}\right) \times \left(0.7855 \frac{\text{g}}{\text{mL}}\right) = 0.393 \frac{\text{g}}{\text{min}}$$

The mass flow rate of acetone fed to the feed side, $m_{\text{acetone, feed}}$, was calculated as 0.393 g/min.

Hence, the mass flow rate of acetone that was retained within the retentate side

$m_{\text{acetone,retentate}}$ will be:

$$m_{\text{acetone,retentate}} = m_{\text{acetone,feed}} - m_{\text{acetone,permeate}}$$

$$m_{\text{acetone,retentate}} = \left(0.393 \frac{\text{g}}{\text{min}}\right) - \left(0.132 \frac{\text{g}}{\text{min}}\right) = 0.261 \frac{\text{g}}{\text{min}}$$

The mass flow rate of acetone retained at the retentate side, $m_{\text{acetone,retentate}}$, was calculated as 0.261 g/min.

To calculate the permeability coefficient, the value of the driving force is required. In this case, the driving force can be written as the difference in partial pressure of acetone on the permeate and the retentate side of the membrane. To calculate the partial pressures of acetone in the CO₂ + acetone flow on the permeate and the retentate side, the mass flow rate of acetone on each side ($m_{\text{acetone,permeate}}$, $m_{\text{acetone,retentate}}$) as well as the mass flow rate of CO₂ on each side ($m_{\text{CO}_2,\text{permeate}}$, $m_{\text{CO}_2,\text{retentate}}$) should be converted to molar flow rate by dividing the value by the molecular weight of acetone (MW_{acetone}) and CO₂ (MW_{CO_2}) respectively. First, the molar flow rate of acetone on the permeate side will be calculated:

$$n_{\text{acetone,permeate}} = \frac{m_{\text{acetone,permeate}}}{MW_{\text{acetone}}}$$

$$n_{\text{acetone,permeate}} = \frac{\left(0.132 \frac{\text{g}}{\text{min}}\right)}{\left(58 \frac{\text{g}}{\text{mol}}\right)} = 0.00228 \frac{\text{mol}}{\text{min}}$$

The molar flow rate of CO₂ on the permeate side will be:

$$n_{\text{CO}_2, \text{permeate}} = \frac{m_{\text{CO}_2, \text{permeate}}}{\text{MW}_{\text{CO}_2}}$$

$$n_{\text{CO}_2, \text{permeate}} = \frac{\left(0.310 \frac{\text{g}}{\text{min}}\right)}{\left(44 \frac{\text{g}}{\text{mol}}\right)} = 0.00704 \frac{\text{mol}}{\text{min}}$$

The acetone mole fraction in the CO₂ + acetone flow on the permeate side will be calculated:

$$y_{\text{acetone, permeate}} = \frac{n_{\text{acetone, permeate}}}{n_{\text{acetone, permeate}} + n_{\text{CO}_2, \text{permeate}}}$$

$$y_{\text{acetone, permeate}} = \frac{\left(0.00228 \frac{\text{mol}}{\text{min}}\right)}{\left(0.00228 \frac{\text{mol}}{\text{min}}\right) + \left(0.00704 \frac{\text{mol}}{\text{min}}\right)} = 0.245$$

The calculation was done the same way for the retentate side. The molar flow rate of acetone on the retentate side will be:

$$n_{\text{acetone, retentate}} = \frac{m_{\text{acetone, retentate}}}{\text{MW}_{\text{acetone}}}$$

$$n_{\text{acetone, retentate}} = \frac{\left(0.261 \frac{\text{g}}{\text{min}}\right)}{\left(58 \frac{\text{g}}{\text{mol}}\right)} = 0.00450 \frac{\text{mol}}{\text{min}}$$

The molar flow rate of CO₂ on the retentate side will be:

$$n_{\text{CO}_2, \text{retentate}} = \frac{m_{\text{CO}_2, \text{retentate}}}{\text{MW}_{\text{CO}_2}}$$

$$n_{\text{CO}_2, \text{retentate}} = \frac{\left(0.0808 \frac{\text{g}}{\text{min}}\right)}{\left(44 \frac{\text{g}}{\text{mol}}\right)} = 0.00184 \frac{\text{mol}}{\text{min}}$$

The acetone mole fraction in the CO₂ + acetone flow on the retentate side will be:

$$y_{\text{acetone, retentate}} = \frac{n_{\text{acetone, retentate}}}{n_{\text{acetone, retentate}} + n_{\text{CO}_2, \text{retentate}}}$$

$$y_{\text{acetone, retentate}} = \frac{\left(0.00450 \frac{\text{mol}}{\text{min}}\right)}{\left(0.00450 \frac{\text{mol}}{\text{min}}\right) + \left(0.00184 \frac{\text{mol}}{\text{min}}\right)} = 0.710$$

Hence, the molar fraction of acetone in the CO₂ + acetone flow on the permeate side, $y_{\text{acetone, permeate}}$, and the retentate side, $y_{\text{acetone, retentate}}$, were calculated as 0.245 and 0.710 respectively.

The partial pressure of acetone on the permeate and the retentate side will be obtained by multiplying the system pressure ($p = 3.21 \text{ MPa}$) with the acetone mole fractions $y_{\text{acetone, permeate}}$ $y_{\text{acetone, retentate}}$ respectively.

$$p_{\text{acetone, permeate}} = p \times y_{\text{acetone, permeate}}$$

$$p_{\text{acetone, permeate}} = (3.208 \text{ MPa}) \times 0.245 = 0.785 \text{ MPa}$$

$$p_{\text{acetone, retentate}} = p \times y_{\text{acetone, retentate}}$$

$$p_{\text{acetone, retentate}} = (3.208 \text{ MPa}) \times 0.710 = 2.28 \text{ MPa}$$

The partial pressure of acetone on the permeate and the retentate side were calculated to be 0.785 MPa and 2.28 MPa respectively.

Hence, the pressure difference of acetone across the membrane $\Delta p_{\text{acetone}}$ can be calculated:

$$\Delta p_{\text{acetone}} = p_{\text{acetone,retentate}} - p_{\text{acetone,permeate}}$$

$$\Delta p_{\text{acetone}} = (2.28\text{MPa}) - (0.785\text{MPa}) = 1.49\text{MPa}$$

Converting the units to cmHg from MPa,

$$\Delta p_{\text{acetone}} = (1.49\text{MPa}) \times \left(\frac{10^6 \text{ Pa}}{\text{MPa}} \right) \times \left(\frac{\text{atm}}{1.013 \times 10^5 \text{ Pa}} \right) \times \left(\frac{76\text{cmHg}}{\text{atm}} \right) = 1119\text{cmHg}$$

The partial pressure difference of acetone across the membrane $\Delta p_{\text{acetone}}$ was calculated to be 1119 cmHg.

Next, the acetone flux was calculated. First, the units of the acetone mass permeation rate, $m_{\text{acetone,permeate}}$, should be converted from mL/min to mL/sec,

$$m_{\text{acetone,permeate}} = \left(0.132 \frac{\text{g}}{\text{min}} \right) \times \left(\frac{\text{min}}{60\text{sec}} \right) = 2.20 \frac{\text{g}}{\text{sec}}$$

Defining mass flux of acetone that permeated through the membrane, $J_{\text{acetone,permeate}}$, as:

$$J_{\text{acetone,permeate}} = \frac{m_{\text{acetone,permeate}}}{A}$$

$$J_{\text{acetone,permeate}} = \frac{\left(2.20 \frac{\text{g}}{\text{sec}} \right)}{\left(2.2\text{cm}^2 \right)} = 1.00 \frac{\text{g}}{\text{sec} \cdot \text{cm}^2}$$

The mass flux of acetone that permeated through the membrane, $J_{\text{acetone,permeate}}$, was calculated as 1.00 g/(sec · cm²).

Converting the units of the membrane thickness $L = 40.6 \mu\text{m}$ to centimeters,

$$L = (40.6\mu\text{m}) \times \left(\frac{\text{cm}}{10^4 \mu\text{m}} \right) = 0.00406\text{cm}$$

Finally, the acetone permeability is calculated as:

$$P_{\text{acetone,permeate}} = \frac{J_{\text{acetone,permeate}} \times L}{\Delta p}$$

$$P_{\text{acetone,permeate}} = \frac{\left(1.00 \frac{\text{g}}{\text{sec} \cdot \text{cm}^2} \right) \times (0.00406\text{cm})}{(1119\text{cmHg})} = 3.63 \times 10^{-6} \frac{\text{g} \cdot \text{cm}}{\text{sec} \cdot \text{cm}^2 \cdot \text{cmHg}}$$

$3.63 \times 10^{-6} \text{ g}/(\text{sec} \cdot \text{cm}^2 \cdot \text{cmHg})$ was obtained as a value for acetone permeability through Teflon AF 1600 film with thickness of $40.6 \mu\text{m}$ and surface area of 2.2 cm^2 at $40 \text{ }^\circ\text{C}$ and 3.21 MPa .

Table 5-3. shows the result along with the experimental condition.

Table 5-3. Acetone permeability through Teflon AF 1600 film with thickness of $40.6 \mu\text{m}$ and surface area of 2.2 cm^2 at $40 \text{ }^\circ\text{C}$ and 3.21 MPa

Pressure [MPa]	CO ₂ permeate flow rate at 40°C, 1atm [mL/min]	CO ₂ retentate flow rate at 40°C, 1atm [mL/min]	Acetone feed flow rate at 25°C [mL/min]	Acetone permeability [g·cm/(sec·cm ² ·cmHg)]
3.21	180	47	0.50	3.63×10^{-6}

CHAPTER 6

PERMEABILITY OF TETRACYCLINE

The permeability of tetracycline through Teflon AF 1600 was measured. The feed side contained a methanol solution in which tetracycline was dissolved. The initial concentration of the solution was approximately 2.9 mg/min. The permeate side was filled with pure methanol. After 24 hours, the solution on the permeate side was analyzed by ultraviolet (UV) spectrophotometry by comparing the absorptivity of the solution with that of pure methanol. As a result, the absorption was the same as the one for pure methanol at 286 nm and 266 nm. Therefore, it can be concluded that there is no permeation of tetracycline through the membrane.

CONCLUSIONS

A membrane set-up to measure the permeability of CO₂ and a set-up to measure the permeability of acetone with CO₂ were designed and built. The latter set-up was verified by checking that 100% of acetone fed was collected at the permeate side in the case without the membrane. Permeation tests were performed for CO₂, acetone and tetracycline. CO₂ permeation was conducted for Teflon AF 2400, AF 1600 and polytetrafluoroethylene (PTFE). CO₂, acetone and tetracycline permeation were conducted for Teflon AF 1600.

The permeability of CO₂ through Teflon AF 2400, AF 1600 and PTFE was measured by monitoring the pressure increase on the permeate side of the membrane while running CO₂ at constant flow rate. The permeability value was obtained for different feed pressures (psig) while maintaining the pressure difference across the membrane at 100 psig. The permeability coefficient decreased in the order Teflon AF 2400 > AF 1600 > PTFE. This is due to the increase of free volume and decrease of the degree of crystallinity in this order. Also the CO₂ plasticization effect on Teflon AF 2400 and AF 1600 were seen. The CO₂ permeability through Teflon AF 2400 became independent of the feed pressure as the polymer was used repeatedly. To a smaller extent, the same effect was seen for Teflon AF 1600, i.e. the CO₂ permeability became less

dependent on feed pressure upon repeated use. Temperature dependence of CO₂ permeability through Teflon AF 2400 was not significant.

The permeability of acetone through Teflon AF 1600 was measured under the condition of having equal CO₂ pressure on the feed and the permeate side of the membrane and conveying acetone to the membrane by flowing with CO₂. The Teflon AF 1600 membrane was found to have a satisfactory permeability of acetone.

The permeability of tetracycline through Teflon AF 1600 was measured by filling the feed side of the membrane with solution of tetracycline dissolved in methanol and the permeate side with pure methanol. It was found that the permeability of tetracycline through Teflon AF 1600 was zero.

Finally, it can be concluded that CO₂ and acetone permeated through Teflon AF 1600 while tetracycline was completely retained. This is a good indication that Teflon AF products would be a suitable choice as a membrane to be used in supercritical antisolvent process where separation of drug from CO₂ and organic solvent is required.

REFERENCES

- Alentiev, A. Y.; Yampolskii, Y. P.; Shantarovich, V. P.; Nemser, S. M.; Plate, N. A. (1997). High transport parameters and free volume of perfluorodioxole copolymers, *J. Membr. Sci.*, 126, 123-132
- Arai, Y.; Sako, T.; Takebayashi, Y. (2002). *Supercritical Fluids: molecular interactions, physical properties, and new applications*, Springer
- Bird, R.; Stewart, W. E.; Lightfoot, E. N. (2002). *Transport phenomena* 2nd edition, John Wiley & Sons, Inc., New York
- Bixler, H. J., Sweeting, O. J. (1971). *The science of technology of polymer films*, Wiley-Interscience, New York
- Bondi, A. (1968). *Physical properties of molecular crystals, liquids and glasses*, Wiley, New York
- Bos, A.; Punt, I. G. M.; Wessling, M.; Strathmann, H. (1999). CO₂-induced plasticization phenomena in glassy polymers, *J. Membr. Sci.*, 155, 67-78
- Brown, W.R., Park, G.S. (1970). *J. Paint. Technol.*, 42, 16
- Buck, W. H.; Resnick, P. R. (1993). Properties of amorphous fluoropolymers based on 2,2-bis(trifluoromethyl)-4,5-difluoro-1,3-dioxole, Paper presented at the 183rd meeting of the electrochemical society, Honolulu, HI
- Carlson, L. H. C.; Bolzan, A.; Machado, R. A. F. (2005). Separation of D-limonene from supercritical CO₂ by means of membranes, *J. Supercritical Fluids*, 34, 143-147

Damle, S.; Koros, W. (2003). Permeation equipment for high-pressure gas separation membranes, *Ind. Eng. Chem. Res.*, 42, 6389-6395

E.W. Lemmon, M.O. McLinden and D.G. Friend, "Thermophysical Properties of Fluid Systems" in NIST Chemistry WebBook, NIST Standard Reference Database Number 69, Eds. P.J. Linstrom and W.G. Mallard, June 2005, National Institute of Standards and Technology, Gaithersburg MD, 20899 (<http://webbook.nist.gov>)

Gupta, R.B.; Chattopadhyay, P. (2003) Method of forming nanoparticles and microparticles of controllable size using supercritical fluids with enhanced mass transfer, US Patent 6,620,351; September 16, 2003.

Higashijima, T.; Ohya, H.; Tsuchiya, Y.; Tokunaga, H.; Aihara, M.; Negishi, Y. (1994). Separation of supercritical fluid mixtures of CO₂ and petroleum components with an asymmetric polyimide membrane, *J. Membr. Sci.*, 93, 165-173

Hu, C. Chang; C.; Ruaan, R.; Lai, J. (2003). Effect of free volume and sorption on membrane gas transport, *J. Membr. Sci.*, 226, 51-61

Krevelen, D. W. (1990). *Properties of Polymers*, 3rd ed., Elsevier, Amsterdam

Merkel, T. C.; Bondar, V.; Nagai, K.; Freeman, B. D.; and Yampolskii, Yu. P. (1999). Gas sorption, diffusion, and permeation in Poly (2,2-bis(trifluoromethyl)-4,5-difluoro-1,3-dioxole-co-tetrafluoroethylene), *Macromolecules*, 32, 8427-8440

Miyashita, T. (2000). *Compact polymer chemistry*, Sankyo Publishers

Mulder, M. (1996). *Basic Principles of membrane technology*, Klumer Academic Publishers, Boston

Nemser, S. M.; Roman, I. C. (1991). Perfluorodioxole membranes, US Pat. 5051114

Patil, V. E.; van den Broeke, L. J. P.; Vercauteren, F. F.; Keurentjes, J. T. F. (2006). Permeation of supercritical carbon dioxide through polymeric hollow fiber membranes, *J. Membr. Sci.*, 271, 77-85

- Peinemann, K.; Schossig, M.; Sartorelli, L.; Kulcke, W.; Brunner, G. (2004). Method for high-pressure gas separation, US Pat. 6755893 B2
- Pinnau, I.; Toy, L. G. (1996). Gas and vapor transport properties of amorphous perfluorinated copolymer membranes based on 2,2-bis(trifluoromethyl)-4,5-difluoro-1,3-dioxole/ tetrafluoroethylene, *J. Membr. Sci.*, 109, 125-133
- Polyakov, A. M.; Starannikova, L. E.; Yampolskii, Yu. P. (2003). Amorphous Teflons AF as organophilic pervaporation materials: Transport of individual components, *J. Membr. Sci.*, 216, 241-256
- Semenova, S. I.; Ohya, H.; Higashijima, T.; Negishi, Y. (1992). Separation of supercritical CO₂ and ethanol mixtures with an asymmetric polyimide membrane, *J. Membr. Sci.*, 74, 131-139
- Schouten, A. E., van der Vegt, A. K. (1987). *Plastics*, Delta Press, The Netherlands
- Spricigo, C. B.; Bolzan, A.; Machado, R. A. F.; Carlson, L. H. C.; Petrus, J. C. C. (2001). Separation of nutmeg essential oil and dense CO₂ with a cellulose acetate reverse osmosis membrane, *J. Membr. Sci.*, 188, 173-179
- Tan, C.; Chiu, Y. (2003). Method for the regeneration of supercritical extractant, US Pat. 6506304 B2
- Taylor, L. T. (1996). *Supercritical fluid extraction*, Wiley-Interscience
- Thakur, Ranjit; Gupta, Ram B. (2005) Rapid Expansion of Supercritical Solution with Solid Cosolvent (RESS-SC) Process: Formation of Griseofulvin Nanoparticles. *Industrial & Engineering Chemistry Research*, 44(19), 7380-7387.
- Verkerk, A. W.; Goetheer, E. L. V.; van den Broeke, L. J. P.; Keurentjes, J. T. F. (2002). Permeation of carbon dioxide through a microporous silica membrane at subcritical and supercritical conditions, *Langmuir*, 18, 6807-6812

Wijmans, J. G.; Baker, R. W. (1995). The solution-diffusion model: a review, *J. Membr. Sci.*, 107, 1-21

Yeo, S.; Kiran, E. (2004). Formation of polymer particles with supercritical fluids: A review, *J. Supercrit. Fluids*